Hybrid Hydrogels for Harnessing Mesenchymal Stem Cell Secretome

by

Victoria A. Sears

A thesis submitted in partial fulfillment
of the requirements for the degree of
Master of Science in Engineering
(Bioengineering)
in the University of Michigan-Dearborn
2019

Master's Thesis Committee:

Associate Professor Gargi Ghosh, Chair
Professor Oleg Zikanov
Associate Professor Joe Fu-Jiou Lo

Acknowledgements

I would like to thank Dr. Gargi Ghosh for her guidance and mentorship in the completion of my thesis. I am also thankful to Malak Nasser for her laboratory training as well as her assistance in aspects of completing this thesis. Further gratitude is extended to lab member Youssef Danaoui for his constant support. I would like to acknowledge and thank Dr. Oleg Zikanov and Dr. Joe Lo for being part of the thesis defense board. In addition, I would like to extend gratitude to the laboratory members of Dr. Argento, Dr. Chakraborty, and Dr. Kanapathipillai for their support and friendship throughout the completion of my research. Finally, I would like to thank the following grant sources for their financial support: NIH (1R03EB026526-01) and NSF (1531217).

Table of Contents

List of Figures

List of Tables

List of Abbreviations

AA	Ascorbic Acid
dECM	Decellularized Extracellular Matrix
DNA	Deoxyribonucleic Acid
DPBS	Dulbecco's Phosphate Buffered Saline
ECM	Extracellullar Matrix
GAGs	Glycoaminoglycans
HUVECS	Human Umbilical Vein Endothelial Cells
iPSCs	Induced Pluripotent Stem Cells
MSCs	Mesenchymal Stem Cells
PEG	Poly(ethylene glycol)

Abstract

The low engraftment and retention rate of mesenchymal stem cells (MSCs) at the target site indicates that the potential benefits of MSC-based therapies can be attributed to their paracrine signaling. In this study, the influence of decellularized extracellular matrices (dECM) on pro-angiogenic signaling of MSC was investigated. Effect of cell passage number on ECM secretion and subsequently, on regulation of MSC secretome was also explored. The study revealed upregulated expression of angiogenesis-related factors upon culturing MSCs on dECMs irrespective of media supplementation. In addition, dECM generated in presence of ascorbic acid promoted expression of angiogenic molecules as compared to dECM derived in absence of media supplementation. Further, it was observed that the effectiveness of dECM to stimulate angiogenic signaling of MSCs was reduced as cell passage number was increased from P3 to P5. The activity of MSC-secreted biomolecules investigated by assessing the proliferation as well as capillary morphogenesis of human umbilical vein endothelial cells (HUVECs) supported the Proteome Profiler data. Working towards the goal of creating a biomaterial capable of recapitulating the multifactorial aspects of the stem cell environment, ECM deposited by MSCs was collected and introduced into alginate solution to create a hybrid material. Alginate concentration was varied while keeping the dECM concentration constant. Swelling ratio, degradation and diffusion of the hybrid hydrogels were explored in comparison to dECM-free (alginate only) gels. Results found that both degradation and diffusion characteristics were impacted by the introduction of matrix proteins. Lastly, the printability of the hybrid hydrogels at various printing pressures was also explored using Cellink's INKREDIBLE bioprinter. Optimal printing pressures for each bioink

composition was explored, and it was revealed that dECM addition improved the bioink's printability at lower printing pressures in comparison to dECM-free gels.

Chapter 1: Introduction

Tissue Engineering

Tissue engineering is an interdisciplinary field that aims to fabricate constructs that can regenerate, maintain, or improve the functions of damaged tissue. The field heavily depends on coalescing cells, bioactive molecules, and biomaterials (scaffolds) to organize tissue restoration and integration with a host environment [1]. Within functional tissues, cells are the main building blocks, secreting its own support structures, referred to as the extracellular matrix (ECM). The ECM not only provides mechanical support for cells, but it also functions as a foundation for interactions with various signaling molecules that elicit and direct cell responses and behaviors (including survival, motility, and growth) [2]. In the field of tissue engineering, researchers try to mimic such interactions by creating a scaffold that hosts cells in presence of biomolecules to promote growth and regeneration.

Throughout the last few decades, research and development in tissue engineering has tackled a wide array of tissue types. Advancements have been made in the regeneration of heart, bone, eye, and many other areas. Even though much progress has been accomplished, further research is still required. Complex organ tissues, such as the lung, have been successfully developed within the laboratory, but the development is at the nascent stage and the clinical study involving transplantation within human body is yet to be initiated [1]. Apart from tissue and organ restoration, this field has been growing in the application of modeling human physiology *in vitro*. The creation of tissue models within the lab allow for researchers to study the complex *in vivo* mechanisms that direct cellular and pathological processes [3]. These tissue engineered models,

by improving the understanding of physiological and pathological processes, permit the development of new drugs. Even further, tissue engineering concepts are also being heavily utilized in cancer research through the fabrication of tumor models to allow researchers to better understand how tumors progress [3].

With the promise of tissue engineering in medical therapeutic advancements, it is crucial for researchers to continue to make progress in the creation of tissues *in vitro*. Towards this, optimization of biomaterials by tailoring its mechanical and regeneration properties for specific applications is crucial. Scaffolds need to be further developed to fully imitate the complex tissue architecture and vascular networks that are found in native tissue.

Biomaterials for Tissue Engineering

As an integral component of tissue engineering, the field of biomaterials is focused on developing materials that encourage cell growth, cell maintenance, and restoration of tissue. Developments in biomaterials are continuing in the direction of promoting regeneration through the utilization of biomechanical, biochemical, and biophysical cues [3]. Biomechanically, this field focuses on mimicking the properties of native ECM as cells are able to sense matrix stiffness and influences their bioactivity. Biochemically, researchers have been encouraging signaling through the binding of growth factors and other important biomolecules to the scaffold to control diffusion, which in turn controls cellular activity and intracellular signaling. Lastly, biophysically, biomaterials are being designed to give anchorage to cells; for example, the introduction of pores within a scaffold allow the cells a place to home as well as pathways to move around [3].

For tissue engineering purposes, polymers, ceramics, composites and metals have all been utilized as biomaterials. Regardless of the type, when determining the suitability of a scaffold to successfully encourage tissue regeneration, different design requirements are to be followed:

1) Biocompatibility: Most importantly, a scaffold must be biocompatible, meaning it does not elicit a toxic or immunological response when exposed to the body. Any inflammatory reaction caused by the biomaterial would be detrimental to the healing process and could induce the host to reject the scaffold.

2) Suitable Mechanical Properties: The biomaterial must provide structural scaffolding that simulates the mechanical properties of the target tissue. Even further, scaffold stiffness can affect cell proliferation and differentiation, so it is an important parameter to study to result in maximal cell expansion *in vivo*.

3) Biodegradability: Since most scaffolds utilized for tissue engineering are not permanent, the material should be engineered to have a degradation rate similar to the tissue regeneration (growth) rate. The tuning of scaffold degradation kinetics is essential to avoid failure in the tissue restoration process. If the rate of degradation is too fast, the scaffold will not be able to support the cells enough before tissue regeneration. On the other hand, if the rate is too slow, it can cause inflammatory responses or necrosis. Lastly, while designing degradability, the by-products must be non-toxic and be easily eliminated from the body [4].

4) Bioactivity: It is essential that the biomaterial can interact with the surrounding environment/tissue in order to encourage cell adhesion, migration, and proliferation. Although not all biomaterials naturally possess a high bioactivity, it can be increased through the addition of biomolecules or proteins that encourage pro-angiogenic signaling and enhanced proliferation cellular responses.

<u>Hydrogels</u>

As one of the more common biomaterials utilized in biomedical applications, hydrogels are water-swollen gels that form 3D hydrophilic, polymeric networks after triggering monomeric units to be crosslinked (chemical reaction, exposure to ultraviolet light, etc). Because of their extremely hydrophilic structure, hydrogels have the capacity to withhold copious amounts of water or fluids. Considering that up to 60% of the human adult body is water [5], this material has incredible potential to be used throughout biomedical applications with its use already prominent in the fields of tissue engineering, drug delivery, and biosensors. Besides its superior hydrophilicity, hydrogels possess other characteristics that make them advantageous biomaterials. Such gels are highly biocompatible and by slightly tuning the composition, cross-linking variables, or other various factors, hydrogels can be fabricated with tunable biodegradability and material properties, such as porosity and mechanical stiffness, to fit applications more accurately.

Hydrogels can be classified based on a number of characteristics due to their high degree of design and fabrication freedom. For instance, hydrogels can be derived from natural (collagen, alginate) or synthetic (poly(ethyleneglycol) diacrylate (PEGDA)) polymers. In tissue engineering applications, there is a slight advantage using natural polymers due to its characteristic of biological recognition [6]. Such materials can also be classified based on their response to environmental stimuli. Conventional hydrogels have a typical swelling behavior when placed in aqueous solutions, but "smart" hydrogels can be designed to exhibit a certain mechanical or swelling behavior in response to certain stimuli, such as temperature, pH fluctuations or an electric field [6]. Lastly, hydrogel durability distinguishes two categories of durable and degradable hydrogels, focusing on their stability in physiological environments.

Briefly, hydrogels can be fabricated to exactly fit specific applications, making them advantageous materials. Throughout tissue engineering, focus has been placed on developing hydrogels to provide structure for cellular organization while tailoring its characteristics to mimic natural tissues. Additionally, emphasis has been placed on creating a highly porous structure to encourage cell ingrowth and aid in the neovascularization of the hydrogel [6]. Most importantly, hydrogels in tissue engineering continue to be improved to better encapsulate and direct cellular functions once implanted in a patient.

Stem Cells in Tissue Engineering

<u>Background</u>

Differing from other various cell types within the human body, stem cells are non-specialized cells, meaning they do not have any structural characteristics to carry out tissue specific functions. Stem cells have the ability to give rise, or differentiate, into specialized cells. For example, depending on the environmental cues, stem cells can be stimulated to differentiate into bone, muscle, or even vascular cells. This characteristic makes them valuable in the field of tissue engineering and regenerative medicine. Further, stem cells have the capacity of self-renewal after long periods of inactivity through cell division. Unlike other cell types that can only proliferate, stem cells can either self-renew to create more stem cells or give rise to specialized cells.

Stem cells have been characterized into three categories, which are distinguished by where they are derived from as well as their differentiation capacity. Briefly, a description of each stem cell type is introduced:

1) <u>Embryonic Stem Cells:</u> These cells are derived from embryos that have developed eggs after being fertilized *in vitro* [7]. They are considered pluripotent stem cells, meaning they possess the ability to differentiate into any cell type in the body.

2) Adult Stem Cells: Considered to be multipotent stem cells, these cells can differentiate into other cell types, but restricted in its ability. Depending on their tissue of origin, they are generally limited to differentiating into more specialized cell types from that tissue or organ [8]. There are adult stem cells in nearly every tissue/organ within the human body. Hematopoietic stem cells and bone marrow stromal (or mesenchymal) stem cells are two examples. Hematopoietic stem cells can form any type of blood cell, where mesenchymal stem cells can generate cartilage, bone, or fat cells [7].

3) Induced Pluripotent Stem Cells (iPSCs): These cells are pluripotent stem cells derived from adult/somatic (terminally differentiated) cells that are reprogrammed through genetic manipulation to the pluripotent state. Because this cell type is a relatively new discovery (2006), it is yet to be determined of the extent that iPSCs are equivalent to embryonic stem cells [8].

Regardless of their type, all stem cells are important in tissue engineering due to their ability to self-renew and to specialize into certain cell lineages when exposed to certain stimuli. Specifically, tissue engineering has focused their efforts in creating functional biomaterials with appropriate characteristics to control stem cell function and differentiation [9]. Throughout this thesis, work was focused on working with and studying mesenchymal stem cells, which will be further elaborated.

Mesenchymal Stem Cells

Mesenchymal stem cells (MSCs) are multipotent, adult stem cells that are critical to the fields of regenerative medicine and tissue engineering. Their ability to differentiate into several diverse cell types and their aptitude to home at injury sites make them prime candidates for clinical therapeutic applications.

The initial discovery of MSCs is credited to the Russian scientist, Alexander Friedenstein. In the 1960s, Friedenstein first isolated a fibroblastic cell type from guinea pig and mouse bone marrow. These cells were found to have a high replicative capacity and could produce multipotential colonies that when heterotopically transplanted, the colonies were capable of generating bone and reticular tissue [10]. Later, in the beginning of the 1990s, Arnold Caplan coined this fibroblastic cell type as "mesenchymal stem cells" and proved that these cells could also generate adipose tissue, cartilage, tendons, and muscle [11].

In addition to their self-renewal properties as elaborated by Friedenstein and Caplan, MSCs were found to impact the surrounding microenvironment through their secretion of numerous growth factors, both autocrine and paracrine. Such released factors decreased inflammation at target sites, enhanced tissue repair, and promoted angiogenesis. Even further, it was discovered that MSC possess high immunosuppressive properties, which permits them to be transplanted into a patient without any prior or after treatment [12].

These groundbreaking discoveries resulted in a pursuit to further investigate the therapeutic potential of MSCs, leading to the development of many cell-based therapies. Such therapies have been developed for the restoration of tissue and organ integrity. Even further, MSC-based therapies are being tested to control numerous diseases, such as diabetes, ischemic heart disease, osteogenesis imperfecta, and various autoimmune diseases (GvHD, Crohn's, Multiple Sclerosis, etc.) [13]. Because of their therapeutic versatility, MSCs remain a significant therapeutic candidate for regenerative medicine and tissue engineering.

Chapter 2: Motivation and Objectives

Even though MSCs show promise for regenerative therapies and tissue engineering applications, there remains a critical problem in the clinical translation of cellular therapy. When MSCs are injected directly into the target site, there is a low retention and engraftment rate due to the harsh microenvironment the cells are subjected to. At such target sites, MSCs can be faced with death promoting stimuli, such as reactive oxygen species, hypoxia, deficiency of extracellular matrix for MSC attachment, and cytotoxic cytokines [14,15]. Thus, the low survival rate of MSCs in such harsh conditions negates the claim that injecting donor MSCs into a patient will result in functional integration with damaged tissue to aid in the restoration process. Overall, this is compromising the utilization of MSC-based therapies.

Alternatively, evidence suggests that bioactive factors secreted by MSCs play a critical role in reparative processes [16-18]. Biomolecules, such as growth factors, angiogenic factors, cytokines, hormones, chemokines, and extracellular matrix proteases, comprise the MSC "secretome" and are potentially involved in MSC-mediated tissue/organ restoration [16-18]. The potential benefits of MSC-secretome span from vascularization, matrix remodeling to anti-inflammatory and anti-fibrotic effects [19-21]. Thus, harnessing MSC secretome can potentially enhance the efficacy of the cellular therapies.

Current methods for modulation of MSC secretome include pharmacological, physiological (hypoxic or anoxic), or growth factor/cytokine pre-conditioning. Some of these pre-conditioning methods are accompanied with genetic manipulations prior to transplantation [22-24]. While these strategies have shown promise in inducing expression and secretion of pertinent

factors, they are limited by transient effects (physiological or pharmacological preconditioning) post-transplantation and by challenges associated with clinical translation due to viral modification of the target gene (genetic manipulation). In addition, none of these pre-conditioning methods can improve the limited engraftment and viability of MSCs *in situ*.

On the other hand, biomaterial-based approaches result in an enhanced control of cells and presentation of MSC secretome [25-32]. Cell encapsulation provides a protective environment for the cells against the components of the immune system while permitting transport of nutrients, oxygen, and released therapeutic factors [33-35]. Several biomaterials, such as alginate, hyaluronan, collagen, fibrin, laminin, and poly (ethylene glycol) (PEG), have been utilized as cell delivery vehicles [36-40]. However, there is a limited capability of these matrices to support cellular viability and function over an extended period of time, which in turn, hinders commercialization of cell-encapsulation-based technologies.

Biomaterials capable of recapitulating the multifactorial aspects of extracellular components of the stem cell environment could enhance the therapeutic capacity of MSCs. The local microenvironment of MSCs, a dynamic "niche", is known to regulate and maintain MSC homeostasis. A significant component of the stem cell niche is the extracellular matrix (ECM) [41], which is comprised of a vast array of collagens, proteoglycans, glycosaminoglycans, and other various structural proteins (fibronectin, elastin, laminin, etc.) that together provides support for cells to function and interact as well as providing a substrate for cell migration [42].

Not only does the ECM provide a mechanical platform, it also supports and regulates various cellular processes through its ability to bind interacting biomolecules, allowing the ECM to mediate in copious biological processes, such as growth factor receptor signaling and chemical signaling pathways. Research has found that ECM controls MSC fate through activating

9

intracellular signaling through adhesion molecules, regulating the activity of soluble and insoluble factors, and implementing mechanical stimulation [41]. For instance, it was found that MSCs cultured on decellularized ECM (dECM) in comparison to being cultured on tissue culture plates resulted in a more prominently induced MSC differentiation (both adipogenic and osteogenic), indicating that the ECM provided cues and signaling pathways to enhance induced differentiation [43].

Due to ECM's critical role in stem cell fate (self-renewal and differentiation), this research hypothesizes that the biochemical cues of ECM influence the paracrine activities of MSCs. Regulating these biochemical cues would permit optimization of MSC-based therapies via improved MSC viability and enhanced harnessing of MSC secretome. Therefore, this work explores the effect of dECM on guiding paracrine activities of MSCs and introduces the idea of developing a bioink based on MSC-derived dECM. Research in this study addressed four objectives, working towards the goal of creating a biomaterial capable of recapitulating the multifactorial aspects of the stem cell environment:

Objective 1: Characterize MSC-derived dECM - The composition of ECM secreted from bone marrow-derived human MSCs was analyzed while also investigating the effect of passage number and ascorbic acid supplementation on its deposition

Objective 2: Explore the effect of dECM on bioactivity and paracrine signaling - MSCs were seeded on top of dECM to study the proliferative activity. Conditioned media from the MSCs seeded on top of dECM was collected, and the concentration of MSC-secreted pro- and anti-angiogenic molecules was determined. The bioactivity of MSC-secreted biomolecules was investigated by assessing the

proliferation as well as capillary morphogenesis of human umbilical vein endothelial cells (HUVECs).

Objective 3: Fabricate hybrid hydrogel - Alginate hydrogels of varying concentrations (2.5%, 5%, and 7%) were synthesized with and without 30 µg/mL of ECM proteins. The impact of ECM addition on the hydrogel's swelling ratio, degradation and diffusion was documented while demonstrating the effects of alginate concentrations.

Objective 4: Test printability of dECM hydrogel – Hybrid hydrogels were printed using Cellink's INKREDIBLE bioprinter. The printed results were imaged and analyzed to explore the printability and optimum printing pressure for each of the bioink concentrations.

Chapter 3: Characterization of dECM

Introduction

The ECM is a complex and dynamic network comprised of a vast array of collagens, proteoglycans, and other various structural proteins (fibronectin, elastin, laminin, etc.) that together provide support for cells to function and interact as well as providing a substrate for cell migration [42]. Because of its complex nature, it is important to characterize the resultant dECM gathered from MSCs that was used throughout all studies within this thesis.

Before exploring dECM components, it was necessary to first confirm that the protocol used for decellularization successfully removed MSCs from their deposited ECM. After such confirmation, experiments were carried out to explore MSC deposition of collagen, fibronectin, and laminin, which are three abundant proteins in ECM. Furthermore, the concentration of glycosaminoglycans (GAGs) deposited by MSCs was investigated. GAGs are also an important component of ECM by regulating cell-matrix interaction through modulating the localization and presentation of growth factors and morphogens [44].

Since culture conditions can strongly influence the deposition and organization of ECM, the impact of ascorbic acid on ECM deposition was investigated in this study. Previous work conducted by Prewitz et al. suggested that ascorbic acid supplementation enhanced the deposition of MSC-derived ECM [45]. Therefore, the influence of culturing MSCs with or without ascorbic acid supplementation on ECM composition was explored.

In addition, to investigate the effect of cell passage on the deposition of ECM MSC passage number was varied from 3 to 5. In an earlier study, compositional changes had been identified

within dECM as a function of MSC age [46]. Studies have also demonstrated dECM derived from low passage cells promotes expansion of primary MSCs; however, dECM generated from aged MSCs loses the potency [46-47]. Taking into account that subcultured cells at different passages deposit ECM with different expression patterns, the effect of these variations on dECM was investigated.

Methods

Preparation and Decellularization of ECM

150,000 MSCs were seeded in each well of 6 well plates. The passages were varied from 3 to 5. Upon confluency, the cells were cultured in normal culture medium with or without ascorbic acid (50 µg/mL, Sigma-Aldrich). After 10 days, the wells were treated with 0.5% Triton-X-100 (Sigma-Aldrich, USA) in 20 mM ammonium hydroxide (NH_4OH, Fischer Scientific, USA) for 10 minutes at 37ºC. Following which the wells were rinsed with Dulbecco's Phosphate Buffered Saline (DPBS, Gibco, New York) for 5 minutes and treated with 200 µ/mL DNase I, RNase-Free (OPTIZYME, Fisher BioReagents), for 60 minutes at 37 ºC. The ECM layers were washed with DPBS and allowed to air dry overnight. Plates were stored at -20ºC until further use.

Confirmation of Decellularized ECM Layers

To confirm decellularization, MSCs were stained with 1% (v/v) Hoechst 33342 (Thermo Scientific, Germany) nucleic acid dye prior to treatment with Triton X-100. Images were captured before and after decellularization via laser scanning confocal microscope (Olympus, FV1200).

DNA Quantification

The amount of DNA present in dECM samples both before and after decellularization and DNase treatment was quantified using Quant-iT™ dsDNA High-Sensitivity Assay Kit (Thermo Fisher, USA). Briefly, DNA was extracted from the samples using papain extraction reagent. To

create the papain extraction solution, 0.1M sodium acetate, 0.01M Na$_2$ETDA (EMD Millipore Corporation, USA), and 0.005M cysteine hydrochloride were added to 0.2M sodium phosphate buffer (sodium phosphate monobasic and sodium phosphate dibasic). Once all the components were completely dissolved, papain suspension (Sigma-Aldrich, USA) was added to the extraction buffer and stored at 4°C for a maximum of 10 days. Papain extraction solution was then added to the samples and incubated at 37°C for 3 h. After digestion, samples and DNA standards were added to a black sided, clear bottom 96 well plate. Working reagent was made per manufacturer's instructions and added to samples/standards. Fluorescence readings were measured using a microplate reader (SpectraMax M3, Molecular Devices) at excitation and emission wavelengths of 480 nm and 530 nm, respectively.

Immunofluorescence

MSCs were cultured on Lab-Tek chamber slides (Thermo Fisher Scientific) and decellularized as described earlier. dECM was fixed using a 50% methanol (Fisher Scientific, Canada) and 50% acetone (Fisher Scientific, USA) solution for 20 minutes at -20°C. Wells were washed with DPBS and blocked with 5% bovine serum albumin (BSA, Sigma-Aldrich, USA) for 1 h at room temperature on an orbital shaker. Samples were rinsed and incubated overnight at room temperature with COL1A1 antibody (Santa Cruz Biotechnology), monoclonal anti-fibronectin antibody (Sigma), or with laminin polyclonal antibody (Thermo Fisher Scientific). Wells were rinsed with DPBS and then incubated with secondary antibodies for 1 h at room temperature. The samples were then rinsed, and confocal images were captured.

Soluble Collagen Assay

The collagen concentration was determined, in collected dECM samples, using Soluble Collagen Assay Kit (Cell BioLabs, Inc., California). Initially, the dECM samples were treated with

0.5 mg/mL of pepsin (Sigma-Aldrich, USA) solution in 0.5 M acetic acid overnight at 4ºC. Digested aliquots were transferred from the wells into a 96 well plate. Following which, the samples and the assay's collagen standards were evaporated to dryness in 37ºC overnight. Sirius Red reagent was added to the samples and collagen standards to stain collagen's triple helix structure, for 1 h as per manufacturer's instructions. The stained wells were washed and incubated with an extraction solution to transfer the eluted dye to a new plate. The amount of collagen was measured using a plate spectrophotometer (Eon, BioTek).

sGAG Assay

Sulfated glycosaminoglycan (sGAG) was quantitatively determined using Glycosaminoglycans Assay Kit (Chondrex, Inc., Washington). sGAG were extracted from the dECM samples using papain extraction reagent, incubating at 37ºC for 3 h. Digested aliquots were collected from the wells and mixed with 1,9 Dimethylmethlyene (DMB) Dye Solution as per manufacturer's instructions. The concentration of GAGs in samples were determined using the Eon plate spectrophotometer and regression analysis.

Results and Discussion

The decellularization method involving treatment with 0.5% Triton X-100 in 20 mM NH$_4$OH proved to be successful according to the images displayed in Figure 1. Prior to treatment, Hoechst staining as well as phase contrast images confirmed confluency with well-defined cell nuclei of MSC cultures (Figure 1 A and B). After treatment, the decellularization solution lysed the MSCs, removing any presence of cell nuclei that was evident in the prior Hoechst stain image. Phase contrast images revealed that the detergent left the ECM layer intact as a web-like, protein network remained at the bottom of the decellularized well.
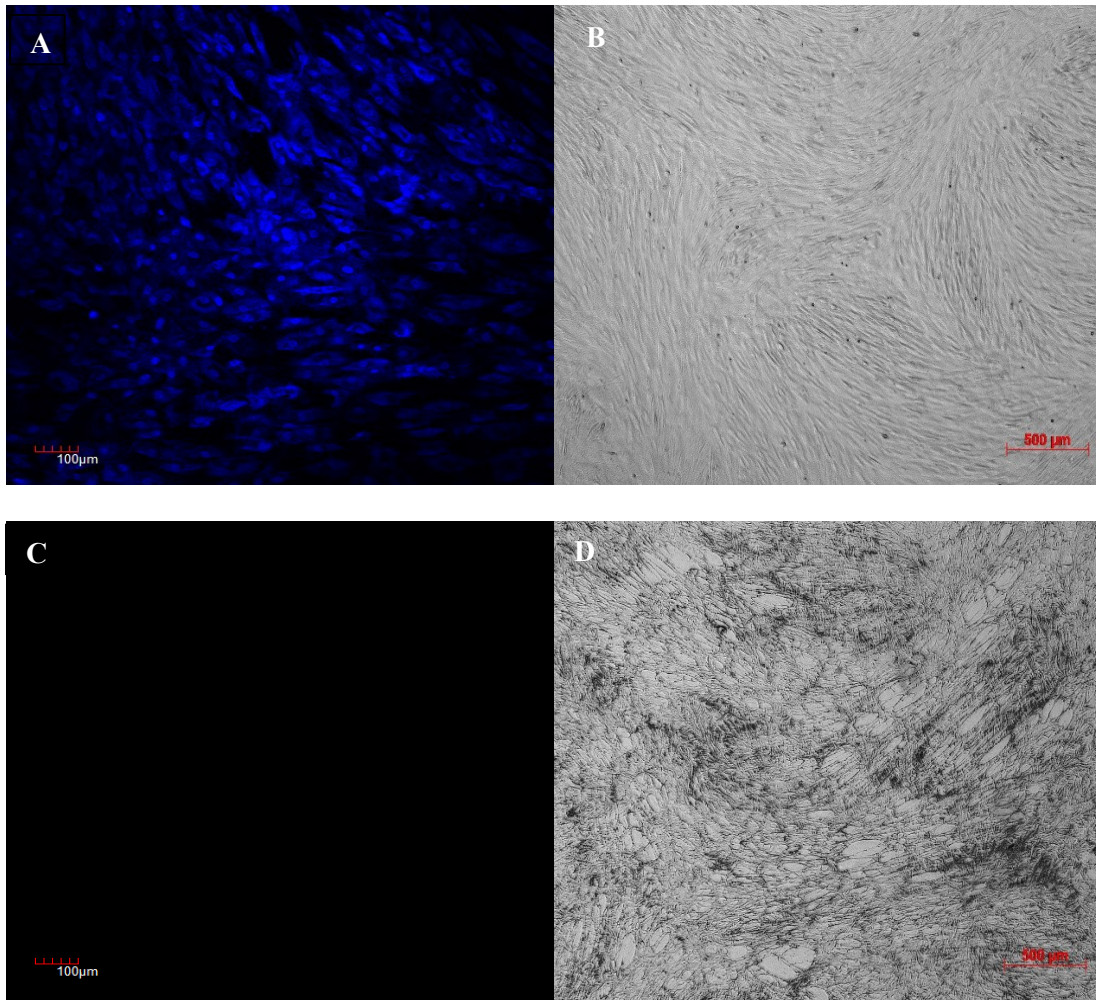
Figure 1. Confirmation of decellularization and deposition of dECM. MSCs were stained with 1% (v/v) Hoechst nucleic acid dye 10 days post-confluence, and images were captured. Hoechst images (scale bar of 100μm) (A) and phase contrast images (scale bar of 500μm) (B) confirmed confluency prior to decellularization. Lack of Hoechst staining confirmed removal of cellular nuclei and genetic material (C), and phase contrast image revealed the remaining deposition of ECM after the removal of cells (D).

Interestingly, DNA quantification indicated that the decellularization process did not rid the matrices of DNA (Figure 2). Quantification of DNA was normalized to the concentration of DNA found in living cells (i.e. before decellularization), which acted as the positive control. After decellularization, around 70% of DNA remained in the ECM that was not treated with DNase. On the other hand, incubation of the matrices with DNase for an hour reduced DNA content in comparison to positive control and dECM without DNA removal.

16
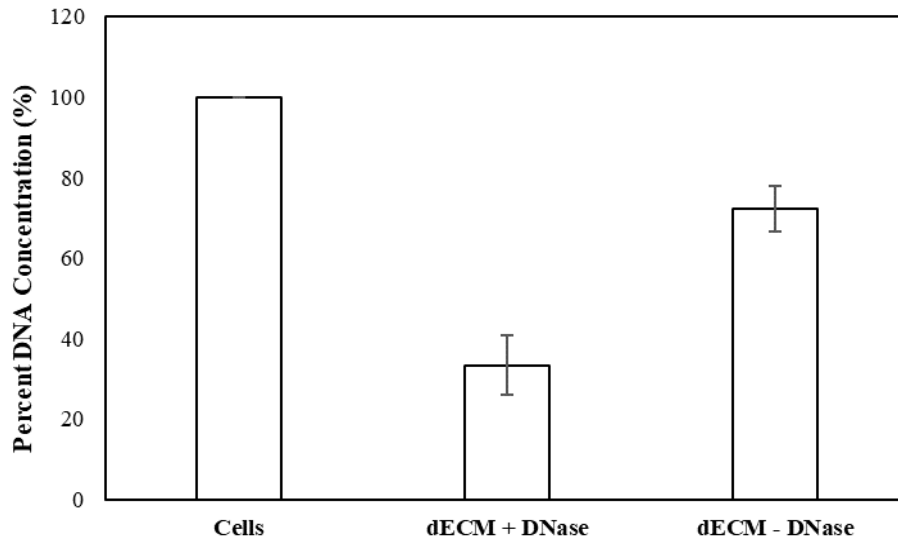
Figure 2. DNA quantification of decellularized matrices. Results presented as percent DNA concentration with respect to the DNA content within the cells prior to decellularization. Quantification was carried out on decellularized matrices treated with DNase (dECM + DNase) and without DNase treatment (dECM-DNase).

Since the decellularization protocol proved to be successful without visibly impacting the ECM, characterization of MSC-derived ECM was carried out. Decellularized matrices generated by MSCs (P4) with and without ascorbic acid supplementation were stained for collagen, fibronectin, and laminin. Immunofluorescence staining (Figure 3) showed that the ECM structural proteins were present in abundance with collagen and fibronectin being more prominent than laminin. In accordance with recent studies [45], this staining demonstrated that ascorbic acid supplementation influenced the secretion and deposition of such ECM components. All three ECM proteins showed an increased deposition when MSCs were supplemented with ascorbic acid during cell culture.
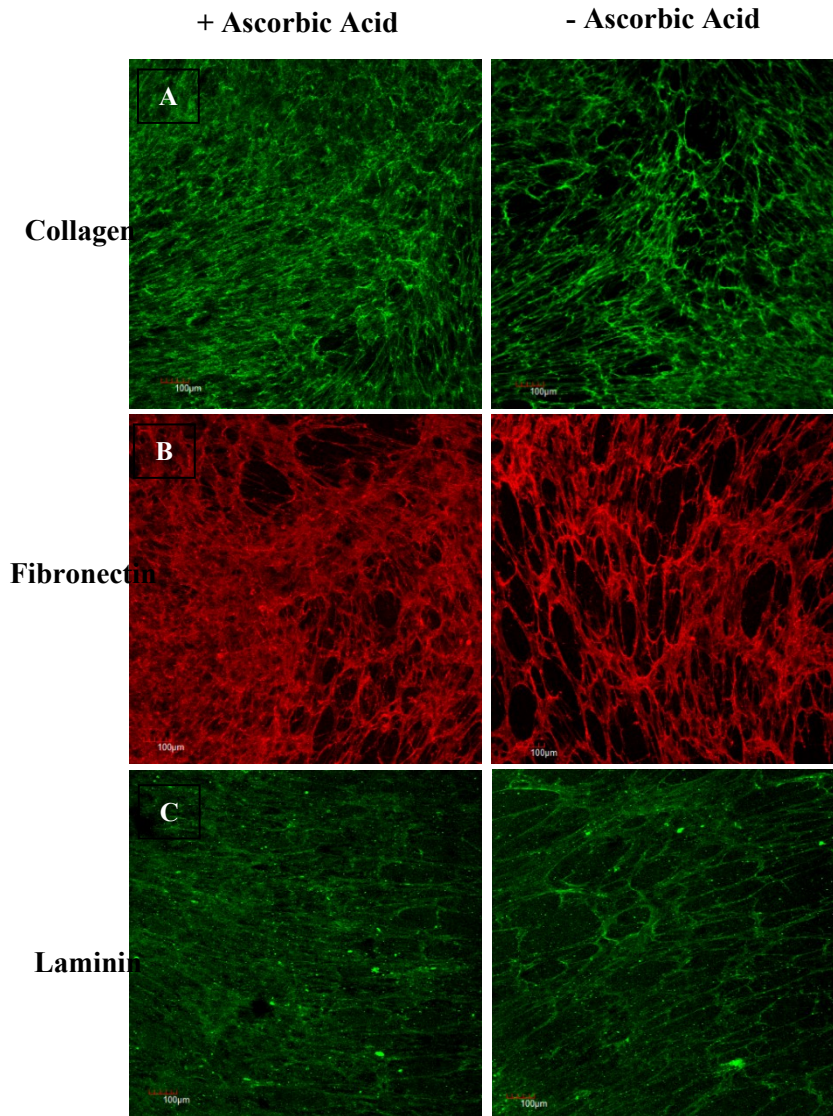
Figure 3. Immunofluorescence staining to compare the effect of ascorbic acid on ECM deposition. MSCs (P4) were decellularized 10 days post-confluence, and cell-free matrices were stained for collagen (A), fibronectin (B), and laminin (C). Scale bar: 100 μm.

In addition to imaging, the concentrations of collagen and GAGs in the deposited matrices was also quantitatively studied while varying media supplementation and passage number (Figure 4). In both assays, a passage-related reduced expression of collagen and GAGs was observed. This observation is in line with earlier studies which demonstrated ECM development is dependent on the passage number of the cells [48]. Further, consistent with other studies, data also demonstrated

an enhanced amount of sulphated GAGs within the secreted matrices in the presence of ascorbic acid. The overall content of GAGs strongly influences the presentation and functionality of growth factors and thus, plays a critical role in the guiding the behavior of adherent cells. However, the enhanced expression was not statistically significant (p-value > 0.05).
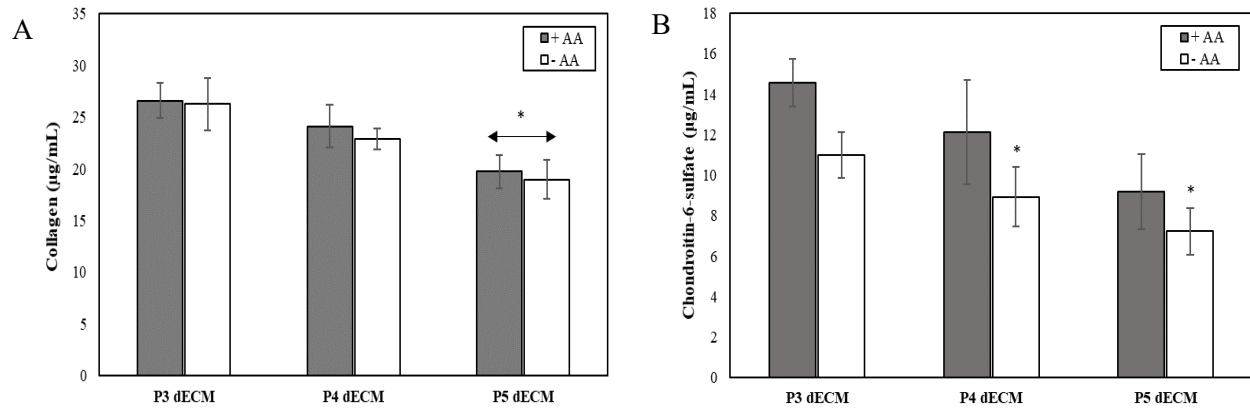
Figure 4. Effect of passage number on the composition of MSC-derived dECM generated with (+AA) or without (-AA) ascorbic acid supplements. Comparison of the deposition of collagen (A) and GAGs (chondroitin-6-sulfate) secretion (B) as a function of cell passage number in the presence and absence of media supplementation. Error bar S.E.M (N=3). *p-value<0.05 with respect to P3 dECM, +AA

Chapter 4: Effect of dECM on Bioactivity and Paracrine Signaling

Introduction

ECM not only provides a highly organized lattice where cells reside and interact with each other, but also plays an important role in regulating the behavior of cells including migratory, proliferative, and metabolic activities [49]. Studies have demonstrated that when cells are cultured on ECM *in vitro*, they display growth characteristics, morphology, as well as biological behaviors which were not observed when harvested on artificial plastic, glass substrate, or TCP coated with isolated ECM components [13]. Studies employing decellularized matrices from epithelial cells, endothelial cells, fibroblasts as well as adult bone marrow stem cells for MSC expansion, corroborated that decellularized matrices offer superior substrates for proliferation of cells in contrast to traditional methods [49-51]. Thus, the following work explores the bioactivity of MSCs when seeded on dECM generated in the presence or absence of ascorbic acid supplements and as a function of passage number.

Although the cell-instructive characteristics of ECM and subsequent effect in regulation of stem cell fate is well known [52], its role in guiding the paracrine signaling of stem cells is still underappreciated. Here, it is explored how dECM impacts MSC paracrine signaling through the investigation of MSC-secreted pro- and anti-angiogenic molecules released in culture media via a human angiogenesis antibody assay. The bioactivity of MSC-secreted biomolecules was then studied by assessing the proliferation as well as capillary morphogenesis (via Matrigel culture) of HUVECs. Effect of passage number and ascorbic acid supplementation on dECM and MSC paracrine signaling was also investigated.

20

Methods

Proliferation Assay of MSCs on dECM

3,000 MSCs (passage 4, P4) were seeded on top of the air-dried dECMs (generated in the presence and absence of ascorbic acid) and cultured in normal culture medium for 48 h. Following which the proliferative activity of the MSCs were measured using XTT Cell Proliferation Assay Kit (ATCC). MSCs seeded on the tissue culture plate (TCP) acted as a control. The proliferation of MSCs on dECMs were expressed as percent growth over the control.

Angiogenesis Profiling of dECM Condition Media

150,000 MSCs (P4) were seeded on air-dried dECM (generated with and without ascorbic acid) in normal culture medium. Cells seeded on TCP acted as a control. After 24 h, the media was replaced with serum-free medium. The spent/conditioned media was collected after 48 h and was stored at -20⁰C until further use. The concentrations of pro- and anti-angiogenic molecules in the conditioned media were determined via Proteome Profiler^{TM} Human Angiogenesis Antibody Array (R&D Systems) as per manufacturer's instructions.

Proliferation of HUVECs

The activity of MSC-secreted biomolecules was investigated by assessing the proliferation of HUVECs. Conditioned media from MSCs (P4) seeded on top of dECMs was collected and concentrated using Vivaspin concentrators (2,000 MWCO, Sartorius). 20,000 HUVECs were seeded in the wells of a 96 well plates in the presence of the conditioned media. HUVECs harvested in presence of normal culture medium acted as control. After 48 h, XTT proliferation assay was utilized to measure proliferative activity of HUVECs.

<u>Capillary Morphogenesis of HUVECs</u>

50 μL of Geltrex ^{TM} LDEV-Free Reduced Growth Factor Basement Membrane Matrix (Gibco) was pipetted into the wells of 96 well plates and incubated at room temperature. 50,000 HUVECs were seeded onto the gels and incubated in the presence of MSC conditioned media and normal HUVECs culture medium at 37 ºC and 5% CO_2. After incubating for 15 h, images of the capillary sprout formations were captured via Zeiss Axio Observer A1 microscope with integrated CCD camera, and the number of sprouts per image was counted.

Results

The influence of dECM, generated as a function of passage number and media supplementation with ascorbic acid, on MSC proliferation was assessed. For the purpose, P4 MSCs were seeded on dECM as culture surfaces and TCP (control). The proliferative activity was measured via XTT proliferation kit. As demonstrated in Figure 5, seeding MSCs on top of dECM increased proliferative activity compared to control. Interestingly, MSCs seeded on P4 dECM, both with or without ascorbic acid, had the highest percent growth (p-value < 0.05).
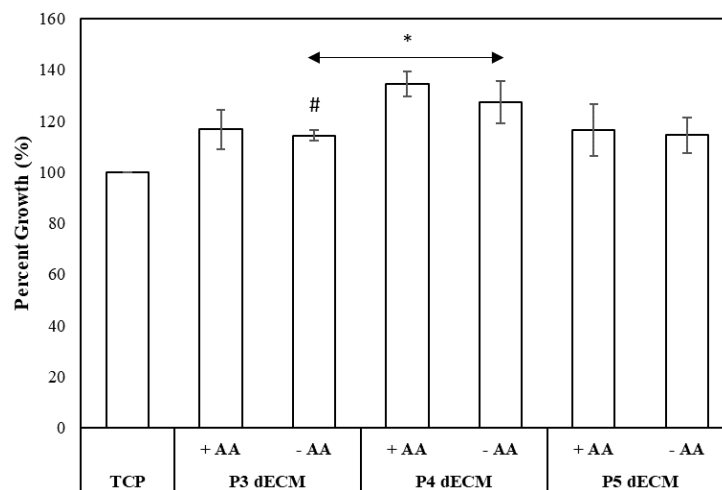
Figure 5. Effect of dECM generated by MSCs (P3-P5) in the presence (+AA) or absence (-AA) of ascorbic acid on proliferation of MSCs (P4). The cell growth was normalized with respect to control (TCP). Error bar S.E.M (N=3). #p-value<0.05 with respect to P4 ECM, +AA; *p-value<0.05 in respect to TCP

To investigate the efficacy of dECM generated by MSCs at different passages with and without media supplementation in promoting angiogenic signaling, MSCs (P4) were seeded on top of dECM (P3-P5). MSCs seeded on TCP (no ECM) acted as the control. The concentration of 55 pro- and anti-angiogenic molecules in the conditioned media was determined using Proteome Profiler[TM] Human Angiogenesis Antibody Array. As demonstrated in Figure 6A and B, compared to the control (no ECM), expression of angiogenesis-related factors was upregulated (relative expression > 1.5) when MSCs were harvested on dECM irrespective of media supplementation for all the passages of MSCs studied. However, the relative expression of different angiogenic molecules varied as a function of passage number of MSCs. Further analysis revealed, dECM generated in presence of ascorbic acid promoted expression of angiogenic molecules as compared to dECM derived in absence of media supplementation (Figure 6C). When the effect of dECM-derived from MSCs of different passages on angiogenic signaling was compared, it was observed that at lower passage number (P3 dECM) the expression of majority of pro-angiogenic molecules were upregulated. The effectiveness of dECM to stimulate angiogenic signaling of MSCs reduced as passage number was increased from P3 to P5.
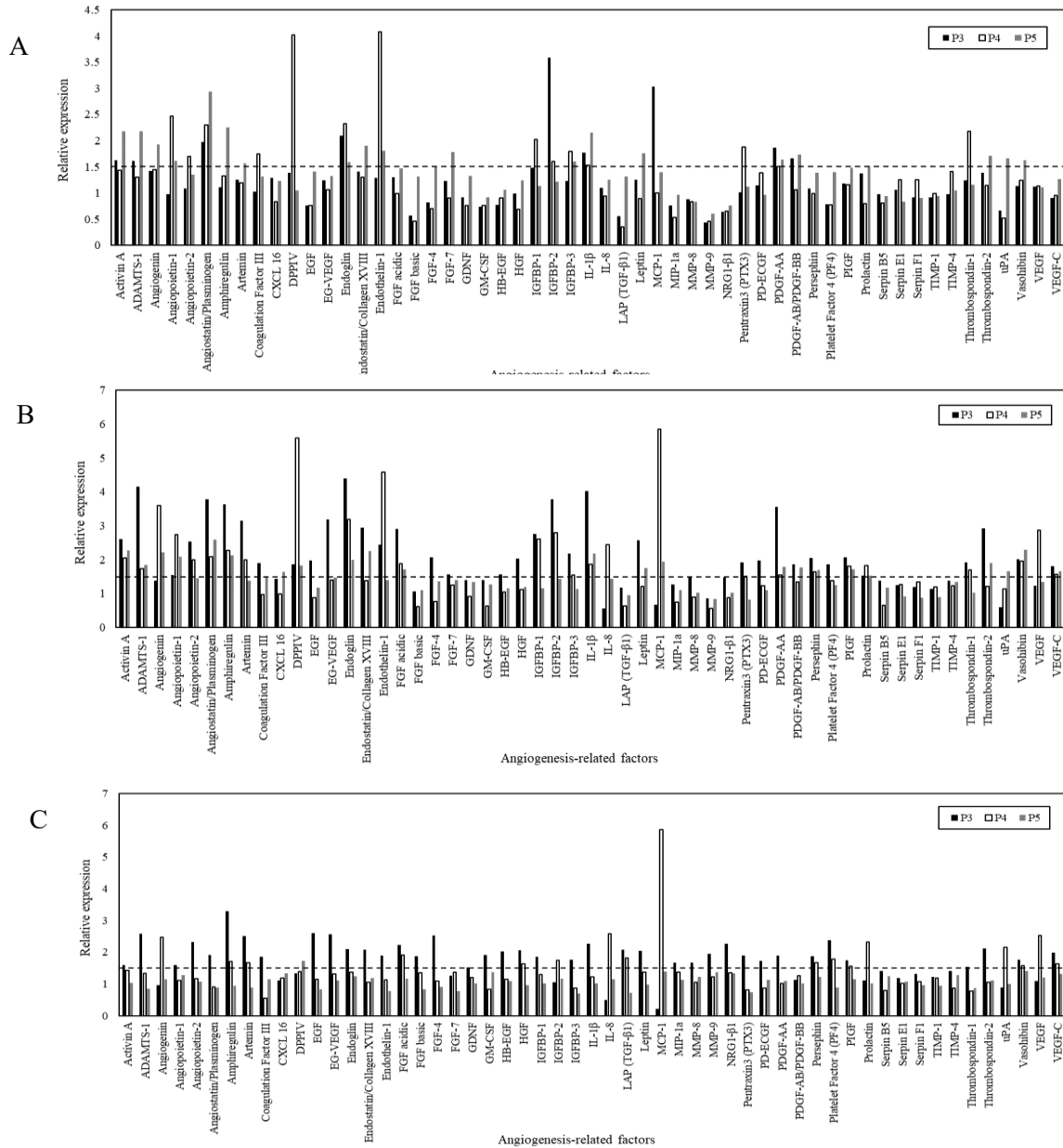
Figure 6. Effect of dECM passage number on angiogenic signaling of MSCs. The expression of angiogenic factors when P4 MSCs were seeded on dECM generated by P3-P5 MSCs in the absence (A) and presence (B) of ascorbic acid relative to TCP (control). The concentration of factors secreted by MSCs seeded on P3-P5 dECM supplemented with ascorbic acid were also normalized to the molecules secreted by MSCs seeded on dECM without ascorbic acid (C). The dotted lines correspond to the relative expression of 1.5

To assess the bioactivity of factors released by MSCs after being seeded on varying dECM passages (P3-P5), the impact of conditioned media on proliferation and capillary morphogenesis of HUVECs was investigated. Endothelial cell culture medium supplemented with growth factors

24

and conditioned media collected from MSCs seeded on TCP (no ECM) acted as the positive and negative controls, respectively. As demonstrated in Figure 7, compared to the negative control, conditioned media collected from MSCs cultured on dECM enhanced proliferation of HUVECs irrespective of passage number and media supplementation. Upon comparing the impact of passage number, maximal proliferation was observed when HUVECs were incubated in conditioned media collected from MSCs seeded on dECM generated by P4 cells (p-value < 0.05).
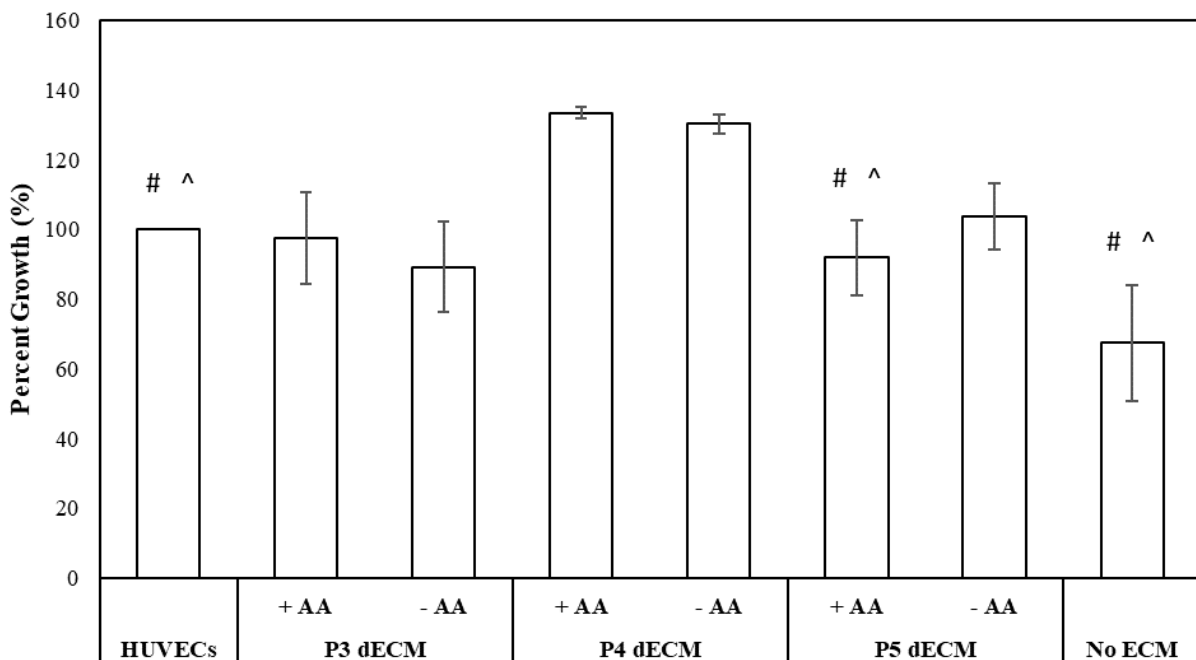
Figure 7. Investigation of activities of factors secreted by P4 MSCs upon seeding on dECM generated by P3-P5 MSCs in the presence (+AA) and absence (-AA) of ascorbic acid. Proliferation of HUVECs in presence of conditioned medium was normalized with respect to HUVECs culture media. Error bar S.E.M (N=3). #p-value<0.05 with respect to P4 dECM, + AA; ^p-value<0.05 with respect to P4 dECM, - AA

To evaluate the influence of MSC-secreted molecules on capillary morphogenesis, the total number of sprouts per image was measured (Figure 8). The conditioned media collected from MSCs seeded on P3 and P4 dECM generated in presence of ascorbic acid stimulated maximal sprouts formation (p-value < 0.05) in comparison to the positive control (HUVECs).
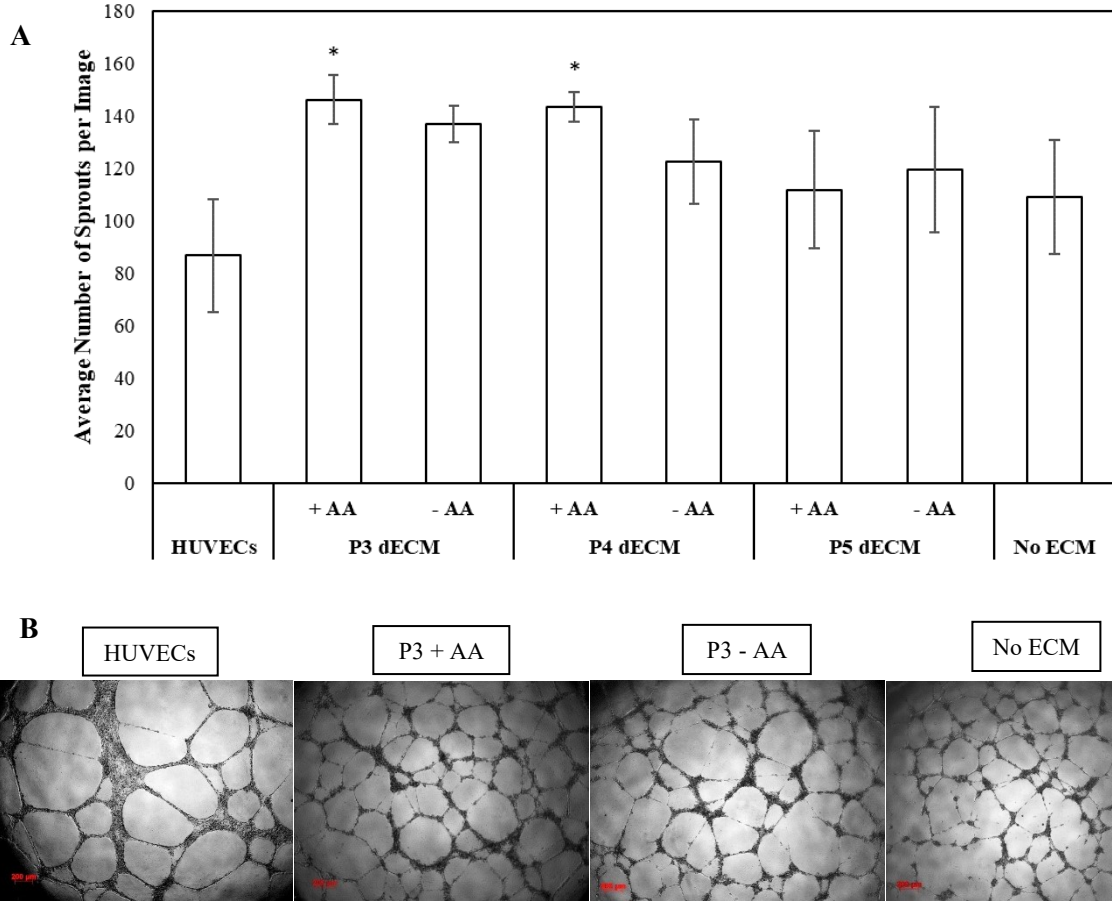
Figure 8. Analysis of activities of factors secreted by P4 MSCs upon seeding on dECM generated by P3-P5 MSCs in the presence (+AA) and absence (-AA) of ascorbic acid. A) Number of sprouts formed per image was measured to assess capillary morphogenesis of HUVECs in presence of conditioned medium. HUVECs culture media was the positive control, and conditioned media collected from MSCs seeded on TCP (no ECM) acted as the negative control. *p-value<0.05 with respect to HUVECs (positive control). B) Typical phase contrast images of the sprouting obtained upon incubating HUVECs with culture medium and conditioned media collected from MSCs seeded on P3 dECM + AA, P3 dECM - AA, and no ECM.

Discussion

In this study, the influence of ECM in stimulating pro-angiogenic activity of MSCs was

explored. The compositional heterogeneity in ECM has been attributed to stem cell fate and thus,

it seems likely that the activity and secretory signature of MSCs will be altered in presence of

ECM with varying biological complexity. To validate the advantages of employing MSC-derived

ECM in regulating the behavior of stem cells, P4 MSCs were harvested on dECM generated in the presence or absence of ascorbic acid. In this work, consistent with other studies, an enhanced proliferation of MSCs was observed in the presence of dECM compared to TCP [47,53]; however, no difference was observed between dECMs as a function of media supplementation. Interestingly, maximal cell growth was observed was dECM generated by P4 MSCs. In contrast to this observation, an earlier study reported better performance of the ECM generated by passage 3 cells compared to passage 4 in terms of cell yield [47]. However, this difference in observation can be attributed to utilization of MSCs from different sources. The previous study analyzed the proliferation of adult MSCs on ECM generated by human fetal MSCs, where the presented work focuses on dECM secreted by adult MSCs [47].

Investigation of the influence of dECM on angiogenic signaling of MSCs revealed large variations in secretome profiles as a function of dECM (media supplementation and cell passages). When MSCs were seeded on dECM generated in absence of ascorbic acid, endoglin and PDGF-AA were the only two factors that were upregulated irrespective cell passages. On the other hand, dECM modulation by ascorbic acid upregulated multiple factors including activing-A, ADAMTS-1, amphiregulin, endoglin, endothelin-1, acidic FGF, IL-1β, PDGF-AA, persephin, PIGF, prolactin, and VEGF-C across cell passages albeit with a large variation. Heterogeneous proangiogenic properties of MSCs as a function of tissue origins have been previously reported [54-56]. Studies have demonstrated that MSCs derived from bone marrow and placental chorionic villi exhibited significant therapeutic angiogenic activities compared to those harvested from adipose tissue or umbilical cord [54]. On the hand, studies have also reported that adipose tissue as well as umbilical cord-derived MSCs exhibit better proangiogenic profile than bone marrow-derived MSCs [55-56].

To explore whether the modulated secretome profiles would translate to enhanced proangiogenic activities of MSCs, proliferation of HUVECs in presence of conditioned media was investigated. Irrespective of cell passages and media supplementation, proliferation of HUVECs was enhanced as compared to conditioned media collected from MSCs seeded on TCP. As a matter of fact, proliferation of HUVECs was found to be comparable (P3 and P5 ECM with and without ascorbic acid) or higher (P4 ECMs) than the normal HUVEC culture media supplemented with cocktail of growth factors. Enhanced stimulatory activity of MSC-secretome can be attributed to endoglin, one of the factors, which was upregulated irrespective of media supplementation across cell passages. Endoglin, a transmembrane accessory receptor for transforming growth factor-beta (TGF-β), promotes proliferation of endothelial cells by regulating the balance of TGF-β signaling through ALK5 and ALK1 receptors [57]. In addition, angiopoietin-1 (Ang-1) and endothelin-1(ET-1), which were primarily upregulated in MSC secretome obtained from P4 ECMs may contribute to higher proliferation of HUVECs. Ang-1 has drawn attention in clinical applications by virtue of its ability to promote blood vessel reconstruction. Ang-1 has been shown to promote proliferation of endothelial cells through activator protein -1 (AP-1) dependent autocrine production of IL-8 [58].

Chapter 5: Characterization of Hybrid Hydrogels

Introduction

The goal of this research is to fabricate a biomaterial capable of recapitulating the multifactorial aspects of extracellular components of the stem cell environment to improve the therapeutic efficacy of MSCs. Focus was placed on creating a hybrid hydrogel to address this goal. This biomaterial was chosen due to its hydrophilicity, tailorability and structural similarity to native tissue. Hydrogels can be synthesized by a variety of synthetic or natural polymers, and the type should be selected to best fit its target application. In this research, the selected hydrogel polymer to be used as the backbone was alginate.

Alginate, a natural polymer derived from seaweed, is extensively used throughout many biomedical applications due to its low toxicity, low cost, stability, and biocompatibility [59]. One of the most attractive properties of using alginate is its ease of gelation when introduced to an environment with divalent cations. Alginate is a linear polysaccharide that is comprised of 1,4-linked α-L-guluronate (G) and ß-D-mannuronate (M) subunits. Once in contact with cations (calcium, barium, and strontium ions), the cations covalently bind the G blocks to form a "egg-box"-like hydrogel [60]. Depending on the cations used to gel the alginate, it can result in different structural properties. For instance, using barium opposed to calcium will result in more rigid gels [60]. For the purpose of this research, calcium ions were used to stimulate gelation. Because this hydrogel will host stem cells during its application, a rigid gel would not be ideal. Additionally, it has been shown that crosslinking alginate using calcium ions can encourage cell proliferation [61].

In an attempt to fabricate a biomaterial that can better harness the multifactorial aspects of the stem cell environment, this chapter explores the development of hybrid hydrogel by combining ECM from cultured MSCs with alginate hydrogels. The following experiments collected dECM from tissue culture and used this collection to fabricate hydrogels with 30 µg/mL of ECM proteins.

Three main material properties of dECM-alginate hydrogels were characterized in the following experiments. The swelling capacity of hydrogels is an important parameter to analyze because this characteristic controls cell migration and diffusion throughout the hydrogel network. Additionally, in order to have a hydrogel to be successful in tissue regeneration, the biomaterial must be retain its integrity for a long period of time. Thus, degradation of dECM gels was analyzed. Lastly, the diffusion of biomolecules released by MSCs encapsulated within hydrogels is important for tissue regeneration, we also studied the diffusion of macromolecules from the gels. These common hydrogel properties were then compared to dECM-free alginate hydrogels to explore whether incorporation matrix proteins affect the hydrogel properties.

Properties of hydrogels are influenced by the concentration of polymer used. For instance, a previous study demonstrated the variances in material properties (swelling, stiffness and stability) when alginate concentration was varied from 0.5 to 1.5% in order to create optimized hydrogels to support neural growth [62]. Therefore, in addition to introducing dECM into the hydrogels and analyzing their properties, the concentration of alginate was also differed in order to explore the alterations in the material properties. The concentrations of alginate were varied from 2.5% (w/w) to 7% (w/w).

Methods

Collection of dECM

MSCs were cultured in T75 flasks and decellularized as described earlier. dECM was scraped with a cell scraper, transferred into 0.02 N acetic acid (Fisher Scientific, USA), and sonicated to homogenize the contents. Samples were lyophilized, reconstituted in 300 μL DPBS, and the total protein in each sample was quantified with a bicinchoninic acid (BCA) protein assay (Thermo Scientific, USA).

Coomassie Blue

Coomassie blue staining was tested on dECM samples collected and prepared from T75 flasks as described before. Laemmli Sample Buffer (Bio-Rad, USA) supplemented with reducing agent, 2-mercaptoethanol (Sigma-Aldrich, Japan), was added to the samples, heated, centrifuged, and then loaded in Precast Gel (Bio-Rad). Fibronectin (Sigma-Aldrich, USA) was loaded as a protein control. Following electrophoresis, the gels were stained with Coomassie Brilliant Blue (Thermo Scientific). Visualization was carried out with Bio-Rad ChemiDoc system.

Hydrogel Fabrication

Three stock concentrations (2.5%, 5%, 7% (w/w)) of alginate solutions were prepared by diluting alginic acid sodium salt (Alfa Aesar, low viscosity) in H_2O. When making the hydrogels, 200 μL of these alginate solutions were dispensed into the wells of 48 well plates. 0.5M calcium chloride ($CaCl_2$, Alfa Aesar) was added on top of pre-solution in excess (500 μL) to encourage crosslinking and gel formation. Crosslinking was carried out for 5 minutes at room temperature followed which the solution was removed. Gels were then washed with dPBS for 5 minutes. To fabricate hybrid gels, dECM was added to the wells of the already dispensed alginate so as to achieve a final concentration of 30 μg/mL dECM protein per gel. Pre-gel solution was thoroughly

mixed with the dECM aliquot to ensure that matrix proteins are distributed throughout the solution prior to crosslinking. dECM gels were then crosslinked and washed as described before.

Swelling Ratio

Following fabrication in 48 well plates, the hydrogels were incubated in 500 µL of dPBS at room temperature. After three days of incubating, gels were collected, and surfaces were dried off with a kimwipe. The weights of the swollen gels were recorded. The gels were then dried at 50°C for 24 h, and the dry weights were measured. Swelling ratio was calculated from the ratio of wet weight to dry weight.

Degradation

To investigate the integrity of the hydrogels, the initial weights of the gels were recorded post-fabrication (day 0). The gels were then incubated in 500 µL of collagenase (Type I, 2.5 units/mL) and the weights of the gels were measured after 2, 4, 6, and 8 days. Degradation was calculated by taking the ratio of sample weights at different time points to the weights recorded on day 0.

Diffusion

50 µg/mL fluorescein isothiocyanate (FITC)-dextran (150,000 kDA, Sigma Aldrich, USA) was added to pre-polymer solutions to fabricate macromolecule-laden gels. The gels were washed in dPBS for 5 min on an orbital shaker to remove dextran molecules from the gel surfaces. dPBS was then aspirated and stored (t=0). 500 µL of dPBS was then added to each hydrogel, and samples were placed on shaker. dPBS was then collected after 1, 3, 5, and 24 h and replaced with fresh dPBS. Collected samples were analyzed using SpectraMax M3 fluorescence spectrometer.

To determine the mechanism of dextran diffusion through the hydrogels, the release of macromolecules was fitted into Korsmeyer-Peppas model given by the following equation:

$$F = \frac{M_t}{M_0} = k_1 t^n$$

where, F is the fractional release of the molecule, M_t is the amount of dextran released at any time point, M_0 is the total mass of dextran that was encapsulated within the initial hydrogels, k_1 is the kinetic constant, t is the release time, and n is the diffusional exponent. For $n \leq 0.5$, the transport of macromolecules is regulated by diffusion, $0.5 \leq n \leq 0.9$ both by diffusion as well as polymer relaxation/erosion, and for $n \geq 0.9$, the transport of molecules is governed via polymer chain relaxation/erosion. The data fitting was carried out on the first 60% cumulative release when $\frac{M_t}{M_0} = 0.6$. The effective diffusivity (D, cm^2/s) of the molecules is related to the cumulative release by the following equation:

$$\frac{M_t}{M_0} = 4 * (\frac{Dt}{\pi L2})^n$$

Where L is the thickness (cm). The diffusivity can then be related to Korsmeyer-Peppas constants:

$$D = \pi L^2 (\frac{k_1}{4})^{1/n}$$

Results

To confirm that dECM proteins were present in the solution after scraping the matrix off the flasks, Coomassie blue staining was utilized by using fibronectin as the protein control. As seen in Figure 9, faint bands matching those of fibronectin were found in the reconstituted dECM solutions collected from P3-P5 MSCs.
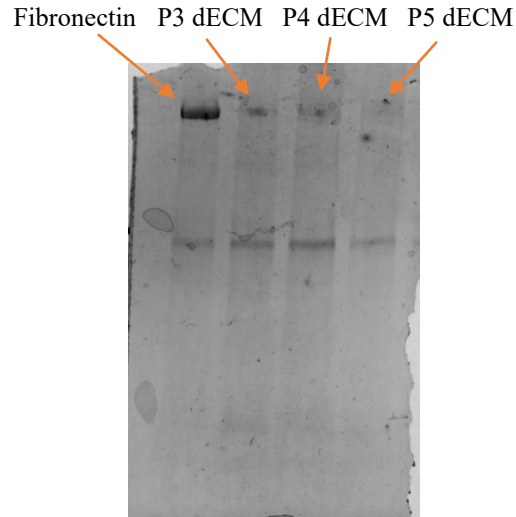
Figure 9. Coomassie blue staining of fibronectin content in collected and reconstituted dECM samples from P3-P5 MSCs. For each sample, faint bands matching to those of the fibronectin control indicate that ECM proteins were successfully collected off of cell culture flask.

Images were captured of the fabricated hydrogels to illustrate the morphological and structural differences when introducing dECM into the biomaterial. As depicted in Figure 10 A-C, dECM hydrogels do not exhibit the spherical shape that the dECM-free gels have. This, in turn, greatly affected the gel thickness as measured with a caliper and shown in Figure 10 D-E. For both dECM positive and negative gels, the concentration of alginate did not significantly affect the shape or size.
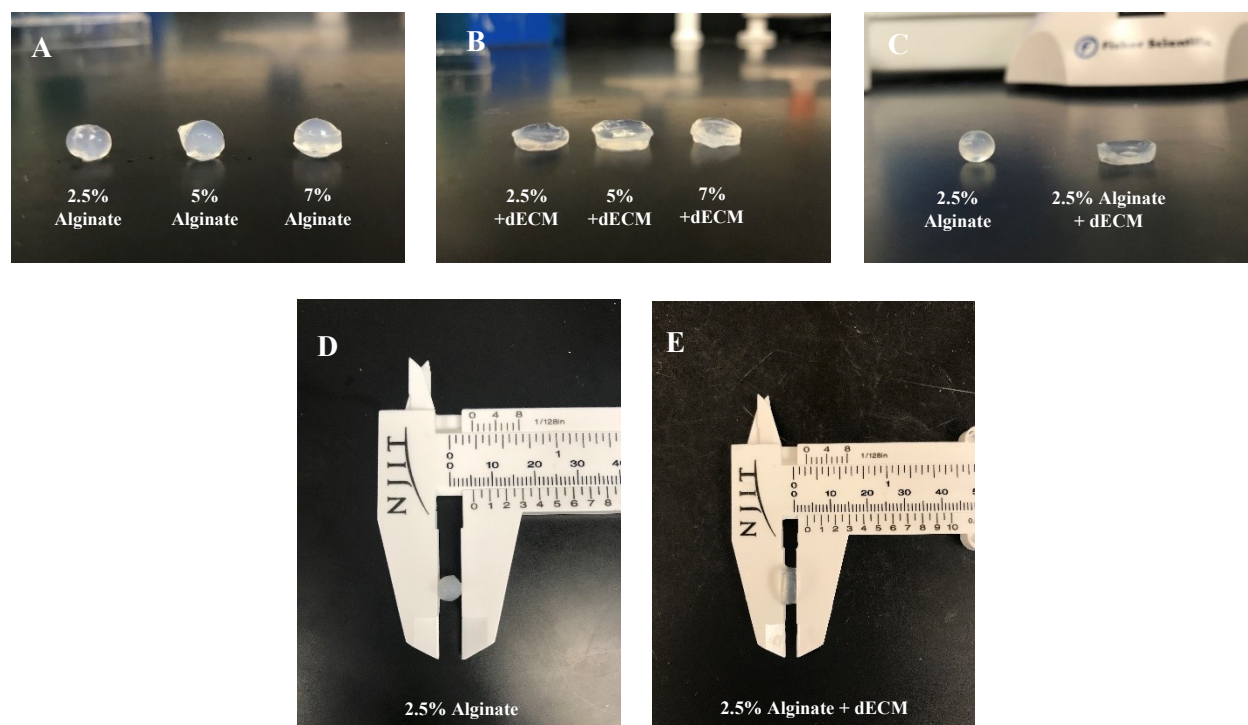
Figure 10. Images of alginate hydrogels fabricated without (A) and with (B) dECM (30 µg/mL). Concentration of alginate used within gels were 2.5%, 5% and 7% (w/w). The addition of dECM within scaffolds disrupted the spherification of hydrogels (C), resulting in less thick gels (D, E). Percent alginate did not impact the shape or size of gels.

The swelling capacity of dECM hydrogels (+dECM) was analyzed by taking the ratio of the weight of the swelled gel over the dry weight. The swelling ratio of hydrogels without dECM (- dECM) was also recorded as a control. As seen in Figure 11, the swelling ratio remained unchanged with the introduction of dECM into the structure. It was also observed that increasing the alginate concentration within the hydrogels decreased its swelling capacity. This is probably because increasing the concentration also increases the number of crosslinks present within the hydrogel network. An increased number of crosslinks limits the hydrogel's capacity for water to infiltrate and swell the gel.
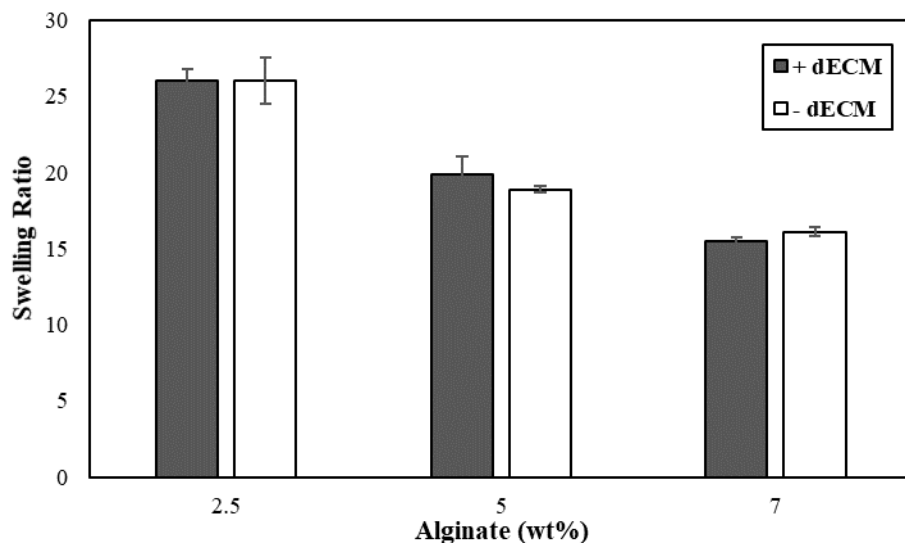
Figure 11. Swelling ratio of alginate hydrogels fabricated with (+dECM) and without (-dECM) dECM. Concentrations of alginate used were 2.5%, 5%, and 7% (w/w). Error bars are the standard deviation of 2 independent experiments.

The integrity of dECM-alginate hydrogels was investigated by incubating the gels in collagenase for a period of 8 days and then analyzing their degradation characteristic (Figure 12). The data is represented as a ratio of sample weights at different time points to the weights recorded on day 0. Results were compared to the degradation of dECM-free alginate hydrogels. Regardless of the alginate concentration and inclusion of dECM, hydrogels were relatively stable throughout the duration of the experiment. 7% alginate hydrogels with and without dECM retained their structure best in comparison to all other gels. In case of 2.5% and 5% alginate hydrogels, the addition of dECM into the scaffold enhanced the integrity of gels as manifested from reduced degradation of the gels compared to gels without dECM.
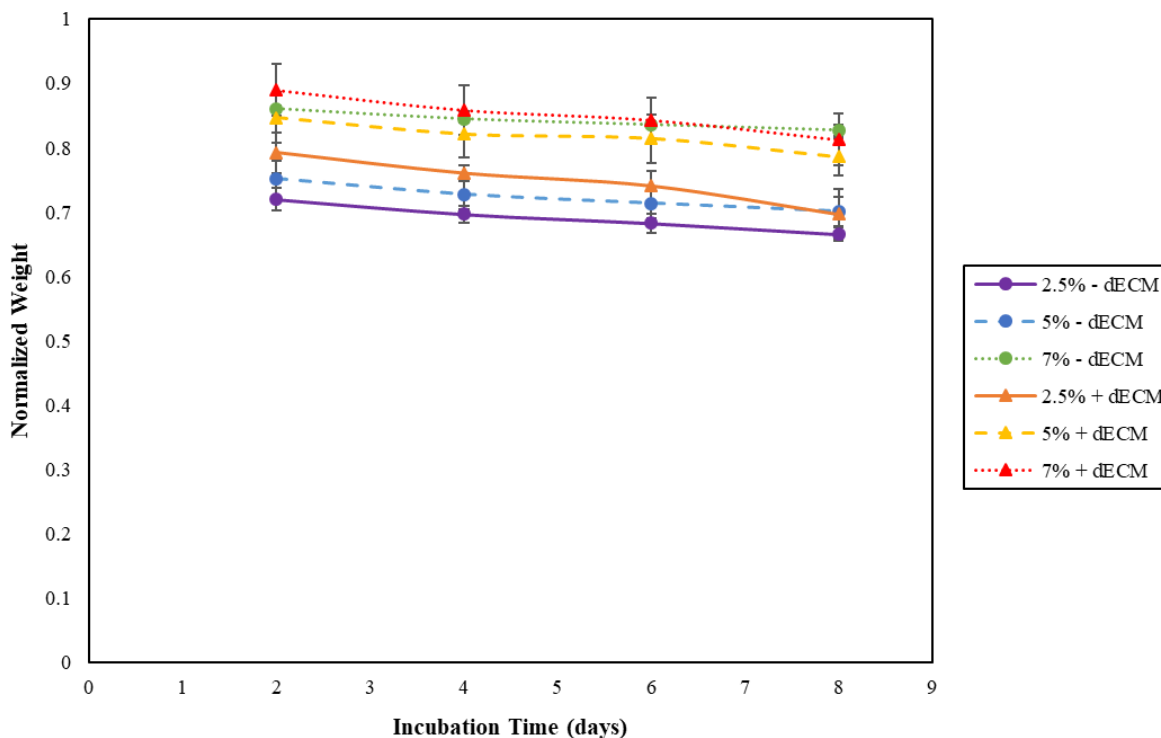
Figure 12. Degradation of alginate hydrogels. Alginate concentrations varied from 2.5%, 5% and 7% (w/w). Hydrogels were also fabricated with (+dECM) and without (-dECM) dECM. Data is presented as a ratio of gel weights at certain time points to the weights recorded on day 0. Error bars are standard deviation.

The diffusivity of macromolecules from dECM-alginate hydrogels was calculated after measuring the concentration of FITC-dextran molecules diffusing out of the gels at certain time points (1, 3, 5, and 24 hours). Figure 13 below depicts the cumulative release of dextran as a function of time. The figure indicates that 2.5% alginate with dECM had the highest diffusion of dextran with around 45% of dextran release during the incubation time of 24 hours. Calculated diffusion coefficients are found in Table 1 below. When comparing the diffusivity of dextran from different dECM hydrogels to hydrogels without the matrix proteins, the inclusion of dECM reduced the diffusion coefficient. The influence of incorporation of dECM was most prominent in the 5% and 7% alginate gels.
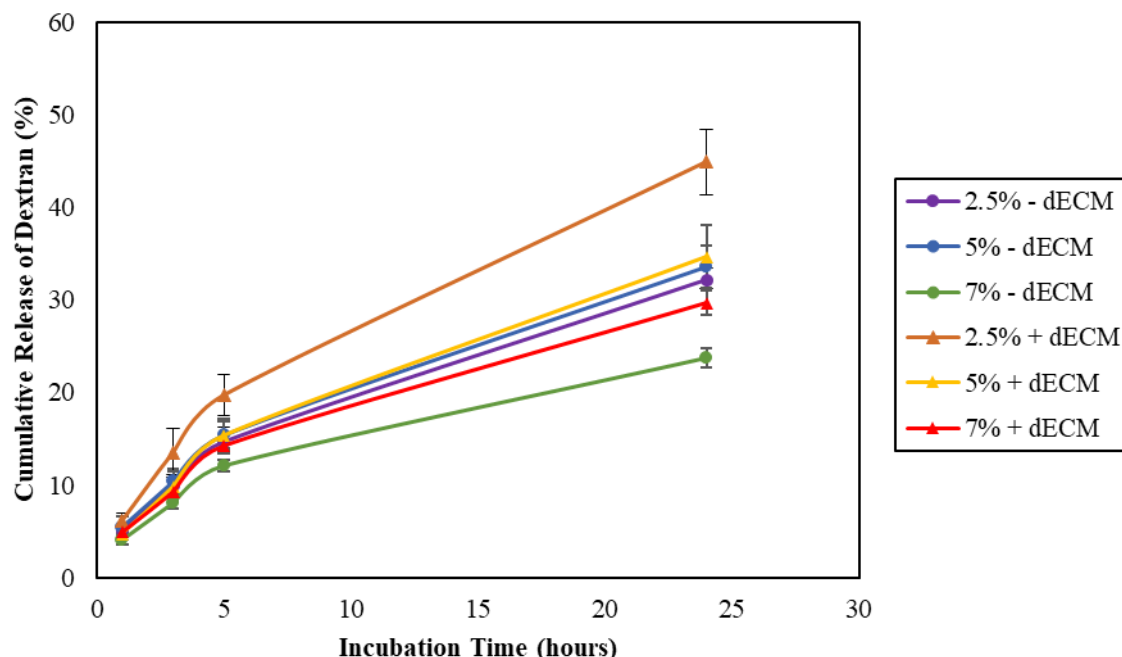
Figure 13. Percentage of cumulative dextran released from alginate hydrogels (2.5%, 5% 7%) made with (+ dECM) and without (- dECM) matrix proteins over an incubation time of 24 hours. Error bars are the standard deviation of the results from three hydrogels per condition.

Table 1. Calculated values of diffusion coefficient of hydrogels. Alginate hydrogels (2.5%, 5%, and 7%) were fabricated with (+dECM) and without (-dECM) 30 µg/mL dECM. Coefficient is presented as average of three hydrogel results ± standard deviation.

Alginate (w/w%)	Diffusion Coefficient (cm²/s)	
	- dECM	**+ dECM**
2.5	1.870±0.578	1.124±0.306
5	2.098±0.806	0.689±0.210
7	1.444±0.282	0.738±0.165

Discussion

Coomassie blue staining revealed that the presence of fibronectin in the dECM samples. It was observed that the intensities of the fibronectin bands were lower for dECM samples collected

from harvesting higher passage MSCs. This corroborates with the previous findings in Chapter 3 that indicated higher passage MSCs deposit lower matrix at reduced concentrations.

Incorporation of dECM with alginate pre-polymer solution interrupted with the spherical structure/droplet formation. Spherification of alginate occurs when the G-blocks interact with cations, creating divalent salt bridges between polymers. Such salt bridges form a thin, but firm outer membrane that induces alginate to construct spheres, leaving the center only partially crosslinked [63]. As illustrated in Figure 10A-E, introducing dECM to alginate resulted in the formation of cylindrical hydrogels as opposed to spheres. It is suspected that surface tension has a role in this alteration of structure.

Next, we investigated the influence of introduction of dECM in different matrix properties including swelling ratio, integrity, and diffusion properties of alginate gels. While increase in alginate concentration reduced swelling ratio of the gels irrespective the presence and absence of dECM. Typically, when hydrogels are placed into an aqueous environment, osmotic driving forces power the influx of fluid into the matrix. Cohesive forces, which are exerted by the hydrogel's polymer strands, resist the expansion of the scaffold, and together, osmotic and cohesive forces create an equilibrium swelling [64]. Generally, the amount of fluid absorbed and extent of swelling capacity is dependent on crosslinking density within the hydrogels. Scaffolds with a high crosslinking density will exhibit a lower swelling capacity than low crosslinked gels [64]. 7% alginate gels with the highest crosslinking density resulted in the lowest swelling ratio. On the other hand, the 2.5% gels had the highest swelling capacity. Interestingly, no difference in the swelling ratio of hybrid and alginate gels was observed. This suggests that dECM is not interrupting the native alginate hydrogel properties.

Investigations into the degradation characteristics of alginate and hybrid gels exhibited relative stability throughout the incubation period of 8 days. All hydrogels maintained 65% or more of its original weight. The hydrogels fabricated with 7% alginate irrespective of dECM displayed the least degradation when comparing to the other alginate concentrations. Further, the degradation results of the 7% alginate gels alluded to be unaffected by the addition of dECM as their results were consistent to each other. On the other hand, the 2.5% and 5% alginate hydrogels suggest a different conclusion. The addition of dECM into the scaffold appeared to enhance the gels durability as less degradation was observed for the 2.5% and 5% gels fabricated with dECM than the gels made without dECM.

The long-term goal is to create MSC-laden scaffolds for efficient tissue restoration. For such a system to work efficiently, transport of bioactive molecules, released by encapsulated MSCs, is critical for recruiting the endogenous cells to the target site. To investigate the transport of marcromolecules from the gels, dextran molecules tagged with FITC as a model molecule was encapsulated with alginate gels and the release was monitored over time. Among all gels, 2.5% alginate with dECM displayed the highest percent release of dextran after 24 hours. Dextran release was fitted into the Korsmeyer-Peppas transport model, which is a simple release mechanism used to describe drug release from a polymeric system [65]. The addition of dECM significantly reduced the diffusivity of dextran from the gels with this outcome being most emphasized for the 5% and 7% alginate gels. Such results suggest that dECM proteins integrated within the alginate matrix could be hindering the ease of diffusion.

Chapter 6: Printability of dECM Hydrogels

Introduction

Three-dimensional (3D) printing, also referred to as additive manufacturing, is a process that builds a 3D object from a computer-aided design (CAD) file using additive processes. Conventionally, an additive process lays down successive layers of material until the 3D object is built. Within this type of manufacturing, there exists a branch called bioprinting that builds 3D scaffolds made of biomaterials, cells, and other biomolecules [66]. This process can be advantageous in the field of tissue engineering because the prints can be designed to selectively deposit cells or biomolecules to fit applications with better precision. Gradients of chemical and biophysical cues can be built into the design to induce and improve regeneration. Further, 3D scaffolds can be printed in precise, complex designs that other conventional fabrication methods cannot achieve. Typical scaffold creation methods, such as electrospinning and gas foaming, cannot accurately control the shape, pore size, and internal network like bioprinting can [67]. Lastly, bioprinting generally uses hydrogels as the material dispensed to create the scaffolds and is termed as a bioink.

Due to the obvious benefits of bioprinting, it was desired to be able to print the hybrid hydrogels developed within this research. Therefore, the printability of the dECM-alginate hydrogels/bioinks was investigated in this chapter. For all concentrations of alginate, images of final prints were captured, and through these images, the printed strand widths, spreading ratio of the bioinks and print accuracy were measured. The bioinks were printed using a pneumatic based extrusion bioprinter called INKREDIBLE. Since this bioprinting method is dependent on pressure,

the following experiment investigated the effect of printing pressure and documented the optimal printing pressure for each bioink.

Methods

Bioprinting Process

Using an INKREDIBLE bioprinter (Cellink, Sweden), all printing was performed at room temperature (25º C). Pre-crosslinked solutions with and without dECM had two drops of food coloring added to them for visual clarity post-print. 2.5% concentrations were stained green, 5% concentrations were stained red, and 7% concentrations were stained blue. Bioinks were then loaded into a 3 mL syringe (BD, USA), and using a female-female luer lock adapter, the inks were transferred into printing cartridges. 25 Gauge (25 G, diameter 0.25 mm) high precision needles were fixed to the end of the cartridges. The pressure was selected to fit both the viscosity of the ink and the needle. Printing speeding was set to 6 mm/s, and prints were dispersed onto a glass petri dish. Print bed and nozzle were homed before every print, setting the zero position for x and y-axes, and the distance between the glass petri dish and the needle was calibrated to give the zero position for the z -axis.

Printability

The printability of alginate hydrogels with and without dECM was analyzed by printing a 10x10mm square with four inner quadrants. The dimensions of the file can be seen in Figure 14 below. Inner and perimeter lines were designed to be 0.25 mm thick. Printing pressure was varied independently for each hydrogel concentration to examine the effects of pressure on printability. The printing pressures used for the 2.5% alginates was 2 and 5 kPa. The printing pressures tested for the 5% alginates was 8, 10, 12, and 15 kPa. Lastly, the pressures examined for the 7% alginates was 12, 14, 18, 24, and 32 kPa. Images of each print were captured, and using ImageJ (NIH, USA),

the dimensions of the printing results were measured. Three tests of printability were examined through the recorded measurements:

1) Printing Accuracy - Knowing the dimensions of the design, printing accuracy was determined by taking multiple width and length measurements of the actual print on ImageJ. These values were then averaged to get an average length of the sides (L_a). The average length of the printed sides was compared to the actual design's side lengths (L) to obtain a printing accuracy. The following equation was used:

$$Printing\ Accuracy\ (\%) = \left(1 - \frac{|L_a - L|}{L}\right) x\ 100$$

2) Strand Width – Multiple measurements of the strand thickness were taken. Measurements were taken from both the inner and perimeter lines. All values were then averaged.

3) Spreading Ratio – Individual strand width measurements were compared to the needle diameter through the following equation. The spreading ratio values per strand width were then averaged for each printed hydrogel and presented with standard deviation.

$$Spreading\ Ratio = \frac{Printed\ Strand\ Width}{Needle\ Diameter}$$
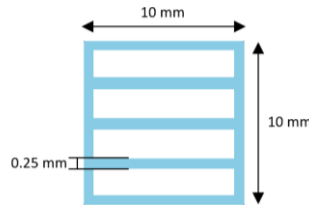
Figure 14. Schematic of the designed structure to test printability.

Results and Discussion

<u>Printability of 2.5% Alginate With and Without dECM</u>

Figure 15 depicts the print outcomes from using 2.5% alginate concentrations as ink. For all cases, the images revealed that this concentration results in a solution that is too liquid-like to be used as a bioink. When the pressure was 2 kPa, one quadrant of the designed structure was visible in the printing of 2.5% alginate with dECM. However, there was quite a bit of pooling, making this condition unprintable. Further, all four quadrants were visible in the print result of 2.5% alginate without dECM, but two minutes post printing, the semi-defined structure settled into a pool of solution. Printing at 5 kPa of pressure, neither the dECM or dECM-free solutions retained the shape it was printed in, resulting in a pool of liquid. Such printing pressure in combination of ink composition was considered unprintable. Therefore, it was concluded that 2.5% alginate concentrations were unprintable despite the addition of dECM and printing pressure.
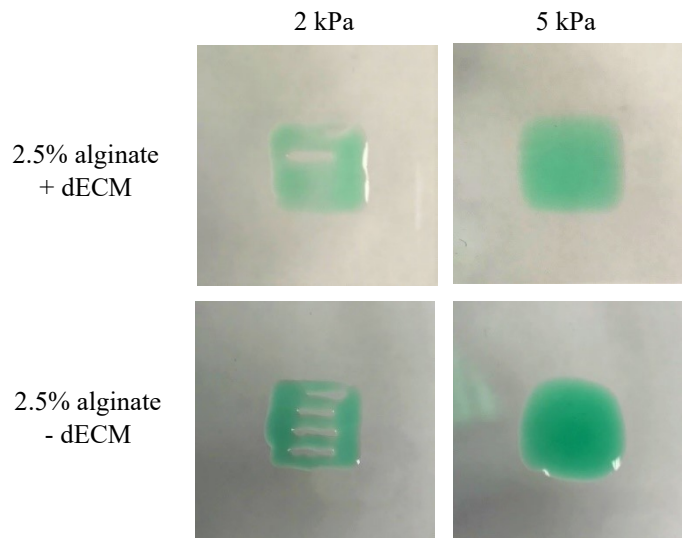
Figure 15. Images of the printed results, using 2.5% alginate with (+dECM) and without (-dECM) ECM proteins. Printing pressure (2 and 5 kPa) was varied to analyze the effect of pressure.

Printability of 5% Alginate With and Without dECM

Unlike the 2.5% alginate concentrations, the 5% gels irrespective of dECM addition showed better printability. Looking at the results in Figure 16, all prints visibly reflected the shape of the design with no obvious failures.
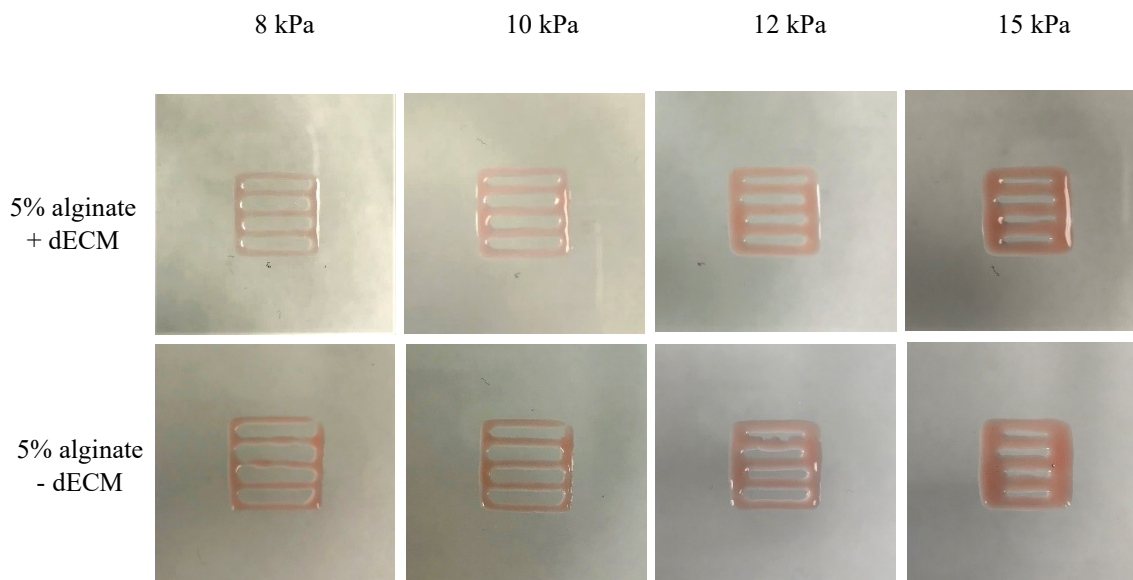
Figure 16. Images of the printed results, using 5% alginate with (+dECM) and without (-dECM) ECM proteins. Printing pressure (8, 10, 12, and 15 kPa) was varied to analyze the effect of pressure on the printability of the inks.

Both visible results and quantitative analysis indicate that increasing the printing pressure results in a thicker printed strand width (Figure 17A). This is expected because at a higher printing pressure, the needle dispenses more material while the print speed stays the same. Comparing the strand widths between the gels with and without dECM, there was no difference, suggesting dECM is not impacting the printability of the material. The spreading ratio indicated the same conclusion as the values remained constant regardless of dECM addition (Figure 17B).
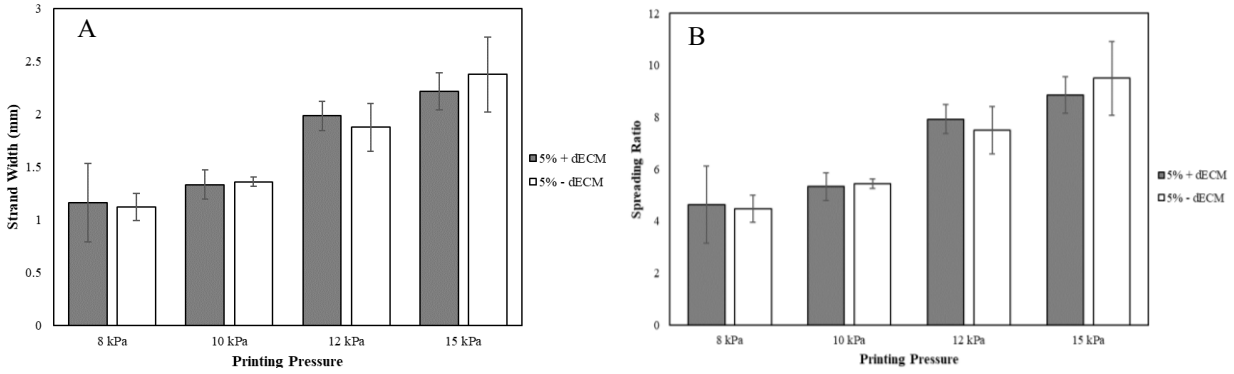
Figure 17. Printabillity of 5% alginate made with (+dECM) and without (-dECM) ECM proteins. A) Average strand widths of the printed structure. B) Spreading ratio of the printed gels to analyze how much the print strand spread in comparison to the original needle diameter. Error bars represent standard deviation.

Table 2 expressed the values of printing accuracy gathered from the outer dimensions of the printed gels. Likewise, the printing accuracies are comparable between the solutions with and without dECM. Focusing on the dECM gels, the printing accuracy, strand width, and spreading ratio suggest that printing at 8 kPa is the optimal printing condition. Print images also support this fact; the lines of the 8 kPa print exhibited a thin and more uniform diameter throughout in comparison to the higher printing pressures. On the other hand, without dECM, the gel printed at 10 kPa exhibited the best printing accuracy, suggesting this condition to be the optimal pressure. Even though the strand width and spreading ratio results of the 10 kPa print were slightly larger in comparison to the 8 kPa print, the images support that 10 kPa is the optimum condition. The dECM-free gel printed at 8 kPa had variable strand widths throughout the print, where the 10 kPa print exhibited more uniform diameters. Therefore, it was concluded that 5% alginate with dECM had the best printability when printed at 8 kPa, and the 5% alginate without dECM proteins printed best at 10 kPa.

Table 2. Calculated values of printing accuracy (%) when varying the printing pressure. The inks compared were 5% alginates with (+dECM) and without dECM (-dECM). Printing accuracy was determined by comparing the printed square's side length to the design's side lengths. Results were expressed as average ± standard deviation.

	Printing Accuracy (%)	
Pressure (kPa)	5% + dECM	5% - dECM
8	55.37 ± 2.29	55.28 ± 1.64
10	50.56 ± 1.80	58.16 ± 0.13
12	48.94 ± 2.51	48.82 ± 1.05
15	34.52 ± 2.02	37.07 ± 3.98

Printability of 7% Alginate With and Without dECM

Examining the printability of 7% alginate inks, a different range of printing pressures had to be selected as opposed to the pressures that were used when printing the 5% concentrations. This is due to the fact that the 7% alginates have a higher viscosity, requiring more pressure for the gel to be dispensed through the fine needle. Thus, the tested printing pressures for the 7% printability analysis were 12, 14, 18, 24, and 32 kPa. Images of the printed constructs, both with dECM and without dECM, can be seen in Figure 18. Initially, it can be observed that the printed gels loaded with dECM are not as thin as the as the printed gels without dECM. However, the dECM-free ink printed at 12 kPa and 14 kPa do not have complete structures; these prints are missing segments, indicating that the printing pressure was too low to allow consistent output of gel from the needles. Both cases were considered to be unprintable, and further printability was not analyzed on these two conditions. Although dECM-free ink was considered to be unprintable at 12 and 14 kPa, the addition of dECM into 7% alginate improved printability at these pressures. A complete structure with uniform line widths were exhibited when dECM gels were printed at 12 and 14 kPa. This effect could be advantageous when introducing cells to the inks. As shown in a previous study, cells are sensitive to high printing pressures due to increased stress that is put on

them [68]. Being able to print the same polymer concentration at lower pressure could possibly improve cell viability in future studies.
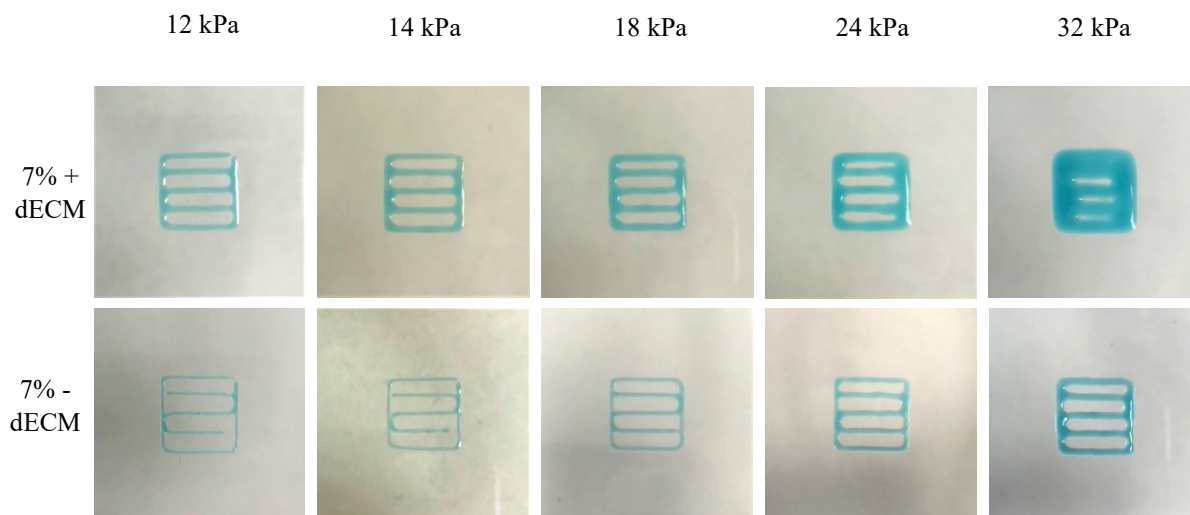
Figure 18. Images of the printed results, using 7% alginate with (+dECM) and without (-dECM) ECM proteins. Printing pressure (12, 14, 18, 24 and 32 kPa) was varied to analyze the effect of pressure on the printability of the inks.

As the images implied and regardless of dECM addition, an increased printing pressure results in thicker strand widths (Figure 19A) and higher spreading ratios (Figure 19B). For all printing pressures, the dECM-free inks exhibited much lower strand widths and spreading ratios than the inks loaded with the ECM proteins. For instance, the inks that were printed at 18 kPa, dECM-alginate gels had a spreading ratio that was over 6 times larger than the needle diameter, whereas the purely alginate gels had a lower spreading ratio of only 2.5 times larger. These results suggest that the dECM is affecting the printability of the 7% alginate gels, which contradicts the results found with the 5% alginate inks.
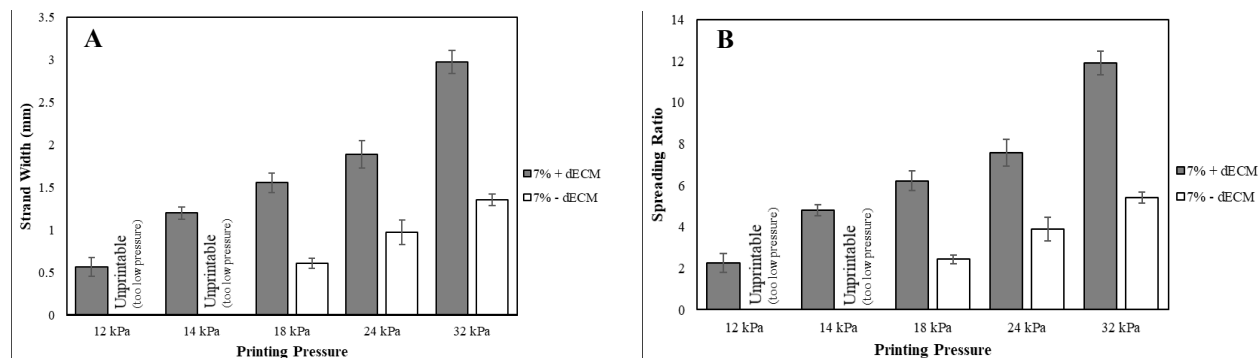
Figure 19. Printabillity of 7% alginate made with (+dECM) and without (-dECM) ECM proteins. A) Average strand widths of the printed structure. B) Spreading ratio of the printed gels to analyze how much the print strand spread in comparison to the original needle diameter. Error bars represent standard deviation.

As expected, the print accuracy also implies that the introduction of dECM into 7% alginate inks is impacting the printability (Table 3). For dECM-free inks, the printing pressure resulting in the best accuracy and overall results was 18 kPa. On the other hand, the ink with dECM addition has its best printability results with a much lower pressure of 12 kPa. Both of these inks expressed relatively same printing accuracy when being printed at their optimal printing pressures. Thus, it can be concluded that the dECM addition is influencing the inks to have improved printability results at lower pressures.

Table 3. Calculated values of printing accuracy (%) when varying the printing pressure. The inks compared were 7% alginates with (+dECM) and without dECM (-dECM). Printing accuracy was determined by comparing the printed square's side length to the design's side lengths. Results were expressed as average ± standard deviation.

	Printing Accuracy (%)	
Pressure (kPa)	7% + dECM	7% - dECM
12	70.38 ± 1.04	Unprintable
14	47.46 ± 0.25	Unprintable
18	46.73 ± 0.01	73.85 ± 2.17
24	44.02 ± 0.77	56.19 ± 0.71
32	27.57 ± 0.80	50.42 ± 1.77

Table 4 below shows the optimum printing pressures and parameters in relation to bioink composition that were found in these experiments. The dECM addition into alginate inks did not influence the print accuracy as both the 5% and 7% alginates with and without matrix proteins respectively exhibited similar accuracy, but just at different printing pressures. It can be seen that the using 5% alginate inks results in a decreased print accuracy in comparison to the 7% inks.

Table 4. Expression of optimal printing parameters with respect to bioink composition.

Bioink		Pressure (kPa)	Nozzle Diameter (mm)	Print Speed (mm/s)	Print Accuracy (%)
+ dECM	2.5	Unprintable			
	5	8	0.25	6	55.37 ± 2.29
	7	12	0.25	6	70.38 ± 1.04
- dECM	2.5	Unprintable			
	5	10	0.25	6	58.16 ± 0.13
	7	18	0.25	6	73.845 ± 2.17

As expressed in Table 4, 5% alginate with dECM exhibited the best printability at 8 kPa, and 7% alginate with dECM printed best at 12 kPa. The strand width, spreading ratio, and images of such prints can be found in Figure 20 below. Even though these were considered the optimal printing conditions for the inks, the spreading ratios indicate that 5% is around 4.5 times the needle diameter and 7% is around 2.25 times the needle diameter. These values may seem extraordinary, but this is to be expected since gravity acts on the dispensed inks, which causes an increase in width compared to needle diameter. Further, 5%-dECM ink exhibited a much higher spreading ratio than 7%-dECM gels. This can be explained by the difference in viscosity. Although the exact viscosity of these dECM-alginate inks is not formally reported in this study, 5% alginate has a lower viscosity due to a less dense crosslinked network and can be confirmed through handling the material during experimentation [69]. Thus, printing with lower viscosity inks creates a more

prominent pooling effect, which explains the larger strand widths for 5%-dECM gels. This effect

can also explain the extreme pooling of 2.5% alginate gels that made that concentration

unprintable. Therefore, due to the viscosity differences, there is a restriction to the minimum

achievable strand width in bioprinting dependent on the material's viscosity. The 5%-dECM gels

may express a thicker width opposed to the 7%-dECM inks, but if printed at lower pressures, their

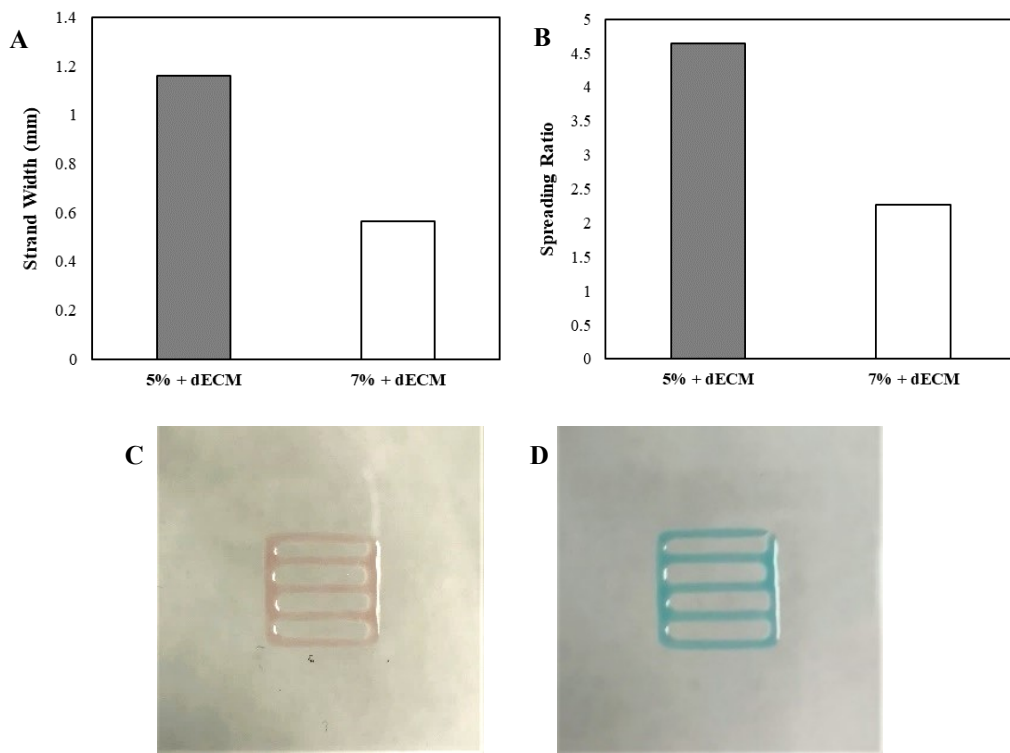structure may not complete, resulting in unprintability.

Figure 20. Comparing printability results of the dECM inks (both 5% and 7% alginate) that were printed at the optimal printing pressures. A) Strand width, B) Spreading ratio, C) 5% alginate with dECM printed at 8 kPa, D) 7% alginate with dECM printed at 12 kPa.

Chapter 7: Conclusion

In this study, MSC-derived matrices were generated under various conditions and characterized to harness the proangiogenic profile of MSCs. dECM secretion under ascorbic acid supplementation resulted in an increased deposition of matrix structural proteins while it was found that increasing passage of MSCs reduces the ECM deposition. Work reports that the presentation and variation of dECM composition alters MSC secretory signatures. dECM generated with media supplementation with ascorbic acid resulted in more upregulated angiogenic signaling of MSCs. dECM-alginate hybrid hydrogels were successfully synthesized with 30 µg/mL of matrix proteins derived from MSCs. Characterizing these gels, swelling ratio showed no difference with and without dECM addition, but indicated an increased swelling for lower alginate concentrations. On the other hand, both degradation and diffusion studies suggest that dECM addition influenced the material properties of the alginate hydrogels. Both the 2.5% and 5% hybrid gels exhibited more resistance to degradation in comparison to the gels without dECM, whereas for all concentrations of alginate, the addition of dECM resulted in a lower effective diffusivity of dextran molecules than the dECM-free counterparts. Printability studies of hybrid hydrogels showed that 2.5% alginate cannot be printed due to its low viscosity. Both the 5% and 7% alginates proved to be successfully printable, and optimum printing pressures were documented. Regardless of dECM addition, 5% alginate showed to have a lower print accuracy and larger spreading ratios when compared to the printability results of 7% alginates. When dECM was introduced into the alginates, the hybrid hydrogels had their optimum prints at lower printing pressures than the

pressures used to print the dECM-free bioinks, which can be advantageous for future studies in

increasing cell viability through the printing process.

Chapter 8: Future Studies

The present work illustrated the composition of MSC-derived dECM from one donor. Future work should analyze the difference in ECM deposition from different donors in order to account for biological variability. We anticipate that there would be some biochemical heterogeneity between matrices deposited by MSCs from different donors, yet they would display consistent composition (i.e. share common set of proteins). Further, dECM composition and its effect on bioactivity of MSCs was studied by varying passage numbers from P3 to P5 and under ascorbic acid supplementation. However, there are other factors that can influence dECM secretion and its impact. For instance, oxygen tension *in vivo* can influence trophic factor secretion of MSCs. Future work involving varying oxygen tension and temporal profiling of angiogenesis related factors (both pro-and anti-angiogenic molecules) will permit elucidating the complex interplay between different microenvironmental factors in guiding angiogenesis.

Addressing the characterization of dECM-alginate hydrogels, a few more experiments need to be carried out. The material properties studied in this work were swelling ratio, degradation, and diffusion, which leaves rheological characterization for future work. Because the end goal is to bioprint these hydrogels into complex, 3D constructs, the material properties need to be explored when the hydrogels are printed to document whether the fabrication process of bioprinting impacts material characteristics. Furthermore, immunostaining of dECM proteins and scanning electron microscope (SEM) images should be taken of printed hydrogels to gather information about the surface topography and composition of the bioinks.

The work completed in this thesis focusing on the bioprinting of hybrid dECM hydrogels were preliminary efforts, and future research is crucial. The fabrication of multi-layered scaffolds needs to be optimized by introducing the crosslinking solution into the second bioprinting nozzle. This would allow for precise crosslinking during the printing process rather than the current method of crosslinking post-print. In addition to this, printing the bioink with cells will be analyzed in future studies through post-printing viability studies. Once the cells are introduced into the dECM-alginate bioinks and successfully printed with, similar experiments exploring paracrine signaling and bioactivity of MSCs will be carried out to study if the hybrid hydrogel improves the therapeutic efficacy of MSCs.

Lastly, the hybrid dECM-alginate hydrogels fabricated within this thesis contained 30 µg/mL of matrix proteins. Further work will vary the dECM concentration within the gels. Experiments will not only study how this impacts the material properties and printability of the bioinks, but work will also address how varying the dECM concentration impacts viability of cells and paracrine signaling of MSCs when the cells are encapsulated within the hydrogel.

References

1. Lee, E. J., Kasper, F. K., & Mikos, A. G. (2014). Biomaterials for tissue engineering. *Annals of biomedical engineering*, *42*(2), 323–337. doi:10.1007/s10439-013-0859-6.

2. (2018). Tissue engineering and regenerative medicine. *National Institute of Biomedical Imaging and Bioengineering*.

3. Castells-Sala, C., Alemany-Ribes, M., Fernandez-Muiños, T., Recha-Sancho, L., Lopez-Chicon, P., Aloy-Reverte, C. … , Semino, C.E. (2013) Current Applications of Tissue Engineering in Biomedicine. *Journal of Bioengineering and Bioelectronics, 2*(4). doi:10.4172/2153-0777.S2-004.

4. Dolcimascolo, A., Calabrese, G., Conoci, S., & Parenti, R. (2019). Innovative Biomaterials for Tissue Engineering. *Biomaterial-Supported Tissue Reconstruction or Regeneration*. doi: 10.5772/intechopen.83839

5. (n.d.). The Water in You: Water and the Human Body. U.S. *Department of the Interior.*

6. El-Sherbiny, I. M., & Yacoub, M. H. (2013). Hydrogel scaffolds for tissue engineering: Progress and challenges. *Global cardiology science & practice*, *2013*(3), 316–342. doi:10.5339/gcsp.2013.38

7. Stem Cell Information Home Page. *Stem Cell Information*. Bethesda, MD: National Institutes of Health, U.S. Department of Health and Human Services, 2016.

8. (2017). What are the different kinds of stem cells. *Americans for Cures*.

9. Mashayekhan, S., Hajiabbas, M., & Fallah, A. (2013). Stem Cells in Tissue Engineering. *Pluripotent Stem Cells*. doi: 10.5772/54371

10. Fitzsimmons, R., Mazurek, M. S., Soos, A., & Simmons, C. A. (2018). Mesenchymal Stromal/Stem Cells in Regenerative Medicine and Tissue Engineering. *Stem cells international*, *2018*, 8031718. doi:10.1155/2018/8031718

11. Bourin, P., Gadelorge, M., Peyrafitte, J. A., Fleury-Cappellesso, S., Gomez, M., Rage, C., & Sensebé, L. (2008). Mesenchymal Progenitor Cells: Tissue Origin, Isolation and Culture. *Transfusion medicine and hemotherapy : offizielles Organ der Deutschen Gesellschaft fur Transfusionsmedizin und Immunhamatologie*, *35*(3), 160–167. doi:10.1159/000124734

12. Park, J. S., Suryaprakash, S., Lao, Y. H., & Leong, K. W. (2015). Engineering mesenchymal stem cells for regenerative medicine and drug delivery. *Methods (San Diego, Calif.)*, *84*, 3–16. doi:10.1016/j.ymeth.2015.03.002

13. Patel, D.M., Shah, J., & Srivastava, A.S. (2013). Therapeutic Potential of Mesenchymal Stem Cells in Regenerative Medicine. *Stem Cells International, 2013*. doi: 10.1155/2013/496218.

14. Rodrigues, M., Griffith, L. G., & Wells, A. (2010). Growth factor regulation of proliferation and survival of multipotential stromal cells. *Stem cell research & therapy, 1*(4), 32. doi:10.1186/scrt32.

15. Song, H., Cha, M.J., Song, B.W., Kim, I.K., Chang, W., Lim, S., … Hwang, K.C. (2010). Reactive oxygen species inhibit adhesion of mesenchymal stem cells implanted into ischemic myocardium via interference of focal adbhesion complex. *Stem Cells, 28*(3), 555-563. doi: 10.1002/stem.302.

16. Horie, N., Pereira, M. P., Niizuma, K., Sun, G., Keren-Gill, H., Encarnacion, A., … Steinberg, G. K. (2011). Transplanted stem cell-secreted vascular endothelial growth factor effects poststroke recovery, inflammation, and vascular repair. *Stem cells (Dayton, Ohio), 29*(2), 274–285. doi:10.1002/stem.584.

17. Liang, X., Ding, Y., Zhang, Y., & Tse, H.F., & Lian, Q. (2014). Paracrine mechanisms of mesenchymal stem cell-based therapy: current status and perspectives. *Cell Transplant 23*(9), 1045-1059. doi: 10.3727/096368913X667709.

18. Williams, A. R., Hatzistergos, K. E., Addicott, B., McCall, F., Carvalho, D., Suncion, V., … Hare, J. M. (2013). Enhanced effect of combining human cardiac stem cells and bone marrow mesenchymal stem cells to reduce infarct size and to restore cardiac function after myocardial infarction. *Circulation*, *127*(2), 213–223. doi:10.1161/CIRCULATIONAHA.112.131110.

19. English, K. (2013). Mechanisms of mesenchymal stromal cell immunomodulation. *Immunology and Cell Biology, 1*(1), 19-26. doi: 10.1038/icb.2012.56.

20. Klinker, M. W., & Wei, C. H. (2015). Mesenchymal stem cells in the treatment of inflammatory and autoimmune diseases in experimental animal models. *World journal of stem cells*, *7*(3), 556–567. doi:10.4252/wjsc.v7.i3.556.

21. Matsui, F., Babitz, S. K., Rhee, A., Hile, K. L., Zhang, H., & Meldrum, K. K. (2017). Mesenchymal stem cells protect against obstruction-induced renal fibrosis by decreasing STAT3 activation and STAT3-dependent MMP-9 production. *American journal of physiology. Renal physiology*, *312*(1), F25–F32. doi:10.1152/ajprenal.00311.2016.

22. Afzal, M. R., Haider, H., Idris, N. M., Jiang, S., Ahmed, R. P., & Ashraf, M. (2010). Preconditioning promotes survival and angiomyogenic potential of mesenchymal stem

cells in the infarcted heart via NF-kappaB signaling. *Antioxidants & redox signaling*, *12*(6), 693–702. doi:10.1089/ars.2009.2755.

23. Kamota, T., Li, T.S., Morikage, N., Murakami, M., Ohshima, M., Kubo, M., … Hamano, K. (2009). Ischemic pre-conditioning enhances the mobilization and recruitment of bone marrow stem cells to protect against ischemia/reperfusion injury in the late phase. *Journal of American College of Cardiology, 53*(19), 1814-1822. doi: 10.1016/j.jacc.2009.02.015.

24. Tang, J.M., Wang, J.N., Guo, L.Y., Kong, X., Yang, J.Y., Zheng, F., … Huang, Y.Z. (2010). Mesenchymal stem cells modified with stromal cell-derived factor 1 alpha improve cardiac remodeling via paracrine activation of hepatocyte growth factor in a rat model of myocardial infarction. *Molecules and Cells, 29*(1), 9-19. doi: 10.1007/s10059-010-0001-7.

25. Jha, A. K., Tharp, K. M., Ye, J., Santiago-Ortiz, J. L., Jackson, W. M., Stahl, A., … Healy, K. E. (2015). Enhanced survival and engraftment of transplanted stem cells using growth factor sequestering hydrogels. *Biomaterials*, *47*, 1–12. doi:10.1016/j.biomaterials.2014.12.043

26. Prestwich G. D. (2013). Delivery, retention and engraftment of progenitor cells in cell therapy. *Biomatter*, *3*(1), e24549. doi:10.4161/biom.24549

27. Gao, J., Liu, R., Wu, J., Liu, Z., Li, J., Zhou, J., … Wang, C. (2012). The use of chitosan based hydrogel for enhancing the therapeutic benefits of adipose-derived MSCs for acute kidney injury. *Biomaterials, 33*(14), 3673–3681. doi: 10.1016/j.biomaterials.2012.01.061.

28. Prestwich, G. D., Erickson, I. E., Zarembinski, T. I., West, M., & Tew, W. P. (2012). The translational imperative: making cell therapy simple and effective. *Acta biomaterialia*, *8*(12), 4200–4207. doi:10.1016/j.actbio.2012.06.043

29. Xiong, Q., Hill, K. L., Li, Q., Suntharalingam, P., Mansoor, A., Wang, X., … Zhang, J. (2011). A fibrin patch-based enhanced delivery of human embryonic stem cell-derived vascular cell transplantation in a porcine model of postinfarction left ventricular remodeling. *Stem cells (Dayton, Ohio), 29*(2), 367–375. doi:10.1002/stem.580.

30. Khetan, S., Katz, J.S., & Burdick, J.A. (2009). Sequential crosslinking to control cellular spreading in 3-dimensional hydrogels. *Soft Matter*, *5*(8), 1601–1606. doi: 10.1039/B820385G

31. Wall, S. T., Yeh, C. C., Tu, R. Y., Mann, M. J., & Healy, K. E. (2010). Biomimetic matrices for myocardial stabilization and stem cell transplantation. *Journal of biomedical materials research. Part A, 95*(4), 1055–1066. doi:10.1002/jbm.a.32904.

32. Unterman, S. A., Gibson, M., Lee, J. H., Crist, J., Chansakul, T., Yang, E. C., & Elisseeff, J. H. (2012). Hyaluronic acid-binding scaffold for articular cartilage repair. *Tissue engineering. Part A, 18*(23-24), 2497–2506. doi:10.1089/ten.TEA.2011.0711.

33. Goren, A., Dahan, N., Goren, E., Baruch, L., & Machluf, M. (2010). Encapsulated human mesenchymal stem cells: a unique hypoimmunogenic platform for long-term cellular therapy. *FASEB Journal: Official Publication of the Federation of American Societies for Experimental Biology, 24*(1), 22-31. doi: 10.1096/fj.09-131888.

34. Chang, T.M. (2005). Therapeutic applications of polymeric artificial cells. *Nature Reviews Drug Discovery, 4*(3), 221-235. doi: 10.1038/nrd1659.

35. Orive, G., Santos, E., Pedraz, J.L., & Hernandez, R.M. (2014). Application of cell encapsulation for controlled delivery of biological therapeutics. *Advanced Drug Delivery Reviews, 67-68*, 3-14. doi: 10.1016/j.addr.2013.07.009.

36. Szot, C.S., Buchanan, C.F., Freeman, J.W., & Rylander, M.N. (2011). 3D in vitro bioengineered tumors based on collagen I hydrogels. *Biomaterials*, *32*(31), 7905-7912. doi: 10.1016/j.biomaterials.2011.07.001

37. Metters, A., & Hubbell, J. (2005). Network formation and degradation behavior of hydrogels formed by Michael-type f reactions. *Biomacromolecules, 6*(1), 290-301. doi:10.1021/bm049607o.

38. Willerth, S. M., Arendas, K. J., Gottlieb, D. I., & Sakiyama-Elbert, S. E. (2006). Optimization of fibrin scaffolds for differentiation of murine embryonic stem cells into neural lineage cells. *Biomaterials*, *27*(36), 5990–6003. doi:10.1016/j.biomaterials.2006.07.036

39. Bae, K.H., Yoon, J.J., & Park, T.G. (2006). Fabrication of hyaluronic acid hydrogel beads for cell encapsulation. *Biotechnology Progress, 22*(1), 297-302. doi: 10.1021/bp050312b

40. Kim, D. H., Martin, J. T., Elliott, D. M., Smith, L. J., & Mauck, R. L. (2015). Phenotypic stability, matrix elaboration and functional maturation of nucleus pulposus cells encapsulated in photocrosslinkable hyaluronic acid hydrogels. *Acta biomaterialia*, *12*, 21–29. doi:10.1016/j.actbio.2014.10.030.

41. Gattazzo, F., Urciuolo, A., & Bonaldo, P. (2014). Extracellular matrix: a dynamic microenvironment for stem cell niche. *Biochimica et biophysica acta*, *1840*(8), 2506–2519. doi:10.1016/j.bbagen.2014.01.010.

42. Kim, S.H., Turnbull, J., & Guimond, S. (2011). Extracellular matrix and cell signalling: the dynamic cooperation of integrin, proteoglycan and growth factor receptor. *Journal of Endocrinology, 209*(2), 139-151. doi: 10.1530/JOE-10-0377.

43. Shakouri-Motlagh, A., O'Connor, A.J., Brennecke, S.P., Kalionis, B. & Heath, D.E. (2017). Native and solubilized decellularized extracellular matrix: A critical assessment of their potential for improving the expansion of mesenchymal stem cells. *Acta Biomaterialia, 55*¸ 1-12. doi: 10.1016/j.actbio.2017.04.014.

44. Couchman, J. R., & Pataki, C. A. (2012). An introduction to proteoglycans and their localization. *The journal of histochemistry and cytochemistry : official journal of the Histochemistry Society*, *60*(12), 885–897. doi:10.1369/0022155412464638.

45. Prewitz, M.C., Stißel, A., Friedrichs, J., Träber, N., Vogler S., Bornhäuser, M., & Werner, C. (2015). Extracellular matrix deposition of bone marrow stroma enhanced by macromolecular crowding. *Biomaterials*, 73, 60-69. doi: 10.1016/j.biomaterials.2015.09.014.

46. Sun, Y., Li, W., Lu, Z., Chen, R., Ling, J., Ran, Q., … Chen, X. D. (2011). Rescuing replication and osteogenesis of aged mesenchymal stem cells by exposure to a young extracellular matrix. *FASEB journal : official publication of the Federation of American Societies for Experimental Biology*, *25*(5), 1474–1485. doi:10.1096/fj.10-161497.

47. Ng, C.P., Sharif, A.R., Heath, D.E., Chow, J.W., Zhang, C.B., Chan-Park, M.B., … Griffith, L.G. (2014). Enhanced ex vivo expansion of adult mesenchymal stem cells by fetal mesenchymal stem cell ECM. *Biomaterials, 35*(13), 4046-4057. doi: 10.1016/j.biomaterials.2014.01.081.

48. Tan, A. R., Alegre-Aguarón, E., O'Connell, G. D., VandenBerg, C. D., Aaron, R. K., Vunjak-Novakovic, G., … Hung, C. T. (2015). Passage-dependent relationship between mesenchymal stem cell mobilization and chondrogenic potential. *Osteoarthritis and cartilage*, *23*(2), 319–327. doi:10.1016/j.joca.2014.10.001.

49. Lin, H., Yang, G., Yan, J., & Tuan, R.S. (2012). Influence of decellularized matrix derived from human mesenchymal stem cells on their proliferation, migration and multi-lineage differentiation potential. *Biomaterials, 33*(18), 4480-4489. doi: 10.1016/j.biomaterials.2012.03.012.

50. DeQuach, J. A., Mezzano, V., Miglani, A., Lange, S., Keller, G. M., Sheikh, F., & Christman, K. L. (2010). Simple and high yielding method for preparing tissue specific extracellular matrix coatings for cell culture. *PloS one*, *5*(9), e13039. doi:10.1371/journal.pone.0013039.

51. Decaris, M. L., & Leach, J. K. (2011). Design of experiments approach to engineer cell-secreted matrices for directing osteogenic differentiation. *Annals of biomedical engineering*, *39*(4), 1174–1185. doi:10.1007/s10439-010-0217-x.

52. Ahmed, M., & Ffrench-Constant, C. (2016). Extracellular Matrix Regulation of Stem Cell Behavior. *Current stem cell reports*, *2*(3), 197–206. doi:10.1007/s40778-016-0056-2.

53. Lai, Y., Sun, Y., Skinner, C. M., Son, E. L., Lu, Z., Tuan, R. S., … Chen, X. D. (2010). Reconstitution of marrow-derived extracellular matrix ex vivo: a robust culture system for expanding large-scale highly functional human mesenchymal stem cells. *Stem cells and development*, *19*(7), 1095–1107. doi:10.1089/scd.2009.0217.

54. Du, W. J., Chi, Y., Yang, Z. X., Li, Z. J., Cui, J. J., Song, B. Q., … Han, Z. C. (2016). Heterogeneity of proangiogenic features in mesenchymal stem cells derived from bone marrow, adipose tissue, umbilical cord, and placenta. *Stem cell research & therapy*, *7*(1), 163. doi:10.1186/s13287-016-0418-9.

55. Amable, P. R., Teixeira, M. V., Carias, R. B., Granjeiro, J. M., & Borojevic, R. (2014). Protein synthesis and secretion in human mesenchymal cells derived from bone marrow, adipose tissue and Wharton's jelly. *Stem cell research & therapy*, *5*(2), 53. doi:10.1186/scrt442.

56. Hsieh, J. Y., Wang, H. W., Chang, S. J., Liao, K. H., Lee, I. H., Lin, W. S., … Cheng, S. M. (2013). Mesenchymal stem cells from human umbilical cord express preferentially secreted factors related to neuroprotection, neurogenesis, and angiogenesis. *PloS one*, *8*(8), e72604. doi:10.1371/journal.pone.0072604.

57. Lebrin, F., Goumans, M. J., Jonker, L., Carvalho, R. L., Valdimarsdottir, G., Thorikay, M., … ten Dijke, P. (2004). Endoglin promotes endothelial cell proliferation and TGF-beta/ALK1 signal transduction. *The EMBO journal*, *23*(20), 4018–4028. doi:10.1038/sj.emboj.7600386.

58. Abdel-Malak, N.A., Srikant, C.B., Kristof, A.S., Magder, S.A., Di Battista, J.A., & Hussain, S.N. (2008). Angiopoietin-1 promotes endothelial cell proliferation and migration through AP-1-dependent autocrine production of interleukin-8. *Blood, 111*(8), 4145-4154. doi: 10.1182/blood-2007-08-110338.

59. Park, H., & Lee, K.Y. (2008). Alginate hydrogels as matrices for tissue engineering. *Natural-Based Polymers for Biomedical Applications, 2008*, 515-532. doi: 10.1533/9781845694814.4.515

60. Kaczmarek-Pawelska, A. (2019). Alginate-based hydrogels in regenerative medicine. *Alginates*. doi: 10.5772/intechopen.88258

61. Venkatesan, J., Bhatnagar, I., Manivasagan, P., Kang, K.H., & Kim, S.K. (2015). Alginate composites for bone tissue engineering: a review. *International Journal of Biological Macromolecules, 72*, 269-281. doi: 10.1016/j.ijbiomac.2014.07.008.

62. Matyash, M., Despang, F., Ikonomidou, C., & Gelinsky, M. (2014). Swelling and mechanical properties of alginate hydrogels with respect to promotion of neural growth. *Tissue Engineering, 20*(5), 401-411. doi: 10.1089/ten.TEC.2013.0252.

63. Lee, P., & Rogers, M.A. (2012). Effect of calcium source and exposure-time on basic caviar spherification using sodium alginate. *International Journal of Gastronomy and Food Science, 1*(2), 96-100. doi: 10.1016/j.ijgfs.2013.06.003.

64. El-Sherbiny, I. M., & Yacoub, M. H. (2013). Hydrogel scaffolds for tissue engineering: Progress and challenges. *Global Cardiology Science & Practice, 2013*(3), 316–342. doi:10.5339/gcsp.2013.38.

65. Dash, S., Murthy, P.N., Nath, L., and Chowdhury, P. (2010). Kinetic modeling on drug release from controlled drug delivery systems. *Acta Poloniae Pharmaceutica, 67*(3), 217-223.

66. Rider, P., Kačarević, Ž. P., Alkildani, S., Retnasingh, S., & Barbeck, M. (2018). Bioprinting of tissue engineering scaffolds. *Journal of Tissue Engineering, 9,* 2041731418802090. doi:10.1177/2041731418802090

67. Gu, B.K., Park, S.J., Kim, Y.J., & Kim, C.H. (2018). 3D bioprinting technologies for tissue engineering applications. *Advances in Experimental Medicine and Biology, 1078*, 15-28. doi: 10.1007/978-981-13-0950-2_2.

68. Nair, K., Gandhi, M., Khalil, S., Yan, K.C., Marcolongo, M., Barbee, K., & Sun, W. (2009). Characterization of cell viability during bioprinting processes. *Biotechnology Journal, 4*(8), 1168-1177. doi: 10.1002/biot.200900004.

69. Guiseppe, M.D., Law, N., Webb, B., A Macrae, R., Liew, L.J., Sercombe, T.B., … Doyle, B.J. (2018). Mechanical behavior of alginate-gelatin hydrogels for 3D bioprinting. *Journal of the Mechanical Behavior of Biomedical Materials, 79*, 150-157. doi: 10.1016/j.jmbbm.2017.12.018.